



HAL
open science

Thrust or detachment? Exhumation processes in the Aegean: Insight from a field study on Ios (Cyclades, Greece)

Benjamin Huet, Loic Labrousse, Laurent Jolivet

► To cite this version:

Benjamin Huet, Loic Labrousse, Laurent Jolivet. Thrust or detachment? Exhumation processes in the Aegean: Insight from a field study on Ios (Cyclades, Greece). *Tectonics*, 2009, 28 (TC3007), pp.1-27. 10.1029/2008TC002397. hal-00401015

HAL Id: hal-00401015

<https://hal.science/hal-00401015>

Submitted on 12 Jan 2022

HAL is a multi-disciplinary open access archive for the deposit and dissemination of scientific research documents, whether they are published or not. The documents may come from teaching and research institutions in France or abroad, or from public or private research centers.

L'archive ouverte pluridisciplinaire **HAL**, est destinée au dépôt et à la diffusion de documents scientifiques de niveau recherche, publiés ou non, émanant des établissements d'enseignement et de recherche français ou étrangers, des laboratoires publics ou privés.

Copyright

Thrust or detachment? Exhumation processes in the Aegean: Insight from a field study on Ios (Cyclades, Greece)

Benjamin Huet,¹ Loïc Labrousse,¹ and Laurent Jolivet¹

Received 24 September 2008; revised 8 February 2009; accepted 6 March 2009; published 16 June 2009.

[1] Whether back-arc extension in the Aegean is symmetric or asymmetric at the regional scale is a key question to the understanding of the dynamics of back-arc extension. New field observations, structural analysis of finite and instantaneous strain, and their relationship with metamorphism on Ios island (Cyclades) lead us to investigate the significance of the South Cycladic Shear Zone (SCSZ). Two successive tectonometamorphic events have been documented in the hanging wall and the footwall of the SCSZ. First, penetrative top-to-the-south shearing is observed in the upper Cycladic Blueschists and the lower Cycladic Basement close to their contact. It is expressed in the hanging wall by shear bands and pressure shadows associated to blueschist facies minerals, contemporaneous with overthrusting of the Cycladic Blueschists over the basement unit. Second, large extensional top-to-the-north shear zones lately crosscut the whole stack. These constraints allow us to reinterpret the kinematics of the Aegean domain during synorogenic and postorogenic periods. When replaced in the reconstructed geometry of the Hellenic Eocene orogenic wedge, the observed top-to-the-south thrusting is coeval with extensional shear zones observed in Syros that could represent the roof of the Cycladic Blueschists. An extrusion structure is then proposed for the exhumation of the Cycladic Blueschists in the subduction zone. Top-to-the-north asymmetric extension together with the Andros-Tinos-Mykonos and Paros-Naxos detachments can be correlated to Oligo-Miocene extension in the back-arc domain. **Citation:** Huet, B., L. Labrousse, and L. Jolivet (2009), Thrust or detachment? Exhumation processes in the Aegean: Insight from a field study on Ios (Cyclades, Greece), *Tectonics*, 28, TC3007, doi:10.1029/2008TC002397.

1. Introduction

[2] The identification of metamorphic core complexes (MCCs) in the Tertiary Basin and Range (western United States) has been a major advance in the study of continental

tectonics [Crittenden *et al.*, 1980; Davis and Coney, 1979]. These extensional structures exhibit metamorphic rocks, ductilely deformed and exhumed below a low-angle normal fault, or detachment. Less metamorphosed rocks, brittlely deformed, lie over the detachment. Such structures have further been recognized in other thinned orogens and especially in the Aegean [Lister *et al.*, 1984]. The MCCs and their detachments are now considered as characteristic features of postorogenic extension.

[3] Moreover, crustal-scale and even lithospheric-scale asymmetric extension has been argued on the basis of dominantly noncoaxial deformation with consistent sense of shear in the MCCs [Wernicke, 1985; Lister and Davis, 1989; Malavieille, 1993]. On the opposite, when several MCCs are present with detachments dipping in opposite directions, the picture may become more symmetrical.

[4] The case of the Aegean Sea is quite exemplary of this discussion. The first description of a cordilleran-type core complex in the Cyclades referred to a south dipping detachment in Naxos and Ios islands [Lister *et al.*, 1984]. Nevertheless, all later papers [e.g., Gautier *et al.*, 1990; Buick, 1991; Faure *et al.*, 1991; Gautier and Brun, 1994a; Jolivet and Patriat, 1999; Mehl *et al.*, 2007], dealing with islands where a detachment showing a clear metamorphic gap between an upper and a lower plate was observed, described the detachments as north dipping and the shear sense in the lower plate as top-to-the-north, even in Naxos. The recent description of top-to-the-south kinematics indicators in the western Cyclades [Grasemann and Petrakakis, 2007] tends to render the overall picture more symmetrical. The tectonic meaning of the major tectonic contact on Ios island described as extensional [Vandenberg and Lister, 1996; Forster and Lister, 1999a] becomes crucial in this discussion. In this paper we have reconsidered this problem after an extensive field survey on Ios. We show that the top-to-the-south movements are not extensional but rather correspond to the thrust of a high-pressure unit on a lower-grade one that was active in the conditions of the blueschist facies and continued to operate during exhumation in the greenschist facies. The whole structure is then reworked by top-to-the-north extensional shear zones operating in the greenschist facies up to brittle conditions.

2. Geodynamic Setting

[5] In the Mediterranean realm, the retreat of the African slab after 35–30 Ma [Jolivet and Faccenna, 2000] has triggered the formation of three back-arc domains within the continental lithosphere previously thickened by Alpine collisions: the Alboran Sea, the Tyrrhenian Sea, and the

¹ISTEP, UMR 7193, Université Pierre et Marie Curie, CNRS, Paris, France.

Aegean Sea from west to east (Figure 1a). During extension, the middle and the lower crust of these basins, ductile deformed, has been exhumed in several metamorphic core complexes separated from the upper crust by detachments. In the MCCs of the Tyrrhenian Sea (Figure 1a), the ductile sense of shear associated to detachments is mainly top-to-the-east [Rossetti et al., 1999; Jolivet et al., 2008]. In the MCCs of the Alboran Sea (Figure 1a), back-arc extension induced the formation of detachments mainly associated to a top-to-the-west kinematics [Augier et al., 2005; Jabaloy et al., 1993; Jolivet et al., 2008; Platt et al., 2006]. In both cases, extension in the middle and lower crust is accommodated at regional scale by asymmetric deformation toward the retreating trench. An important part of the back-arc extension has then been controlled by simple shear arguing for predominant

influence of a basal shear on the extension of the continental crust [Jolivet et al., 2008].

[6] In the Cycladic MCCs of the Aegean Sea (Figures 1a and 1b), recent findings show that no simple trend can be inferred from the distribution of senses of shear. The northern Cycladic detachment (Andros, Tinos, Mykonos, Ikaria) is associated to top-to-the-north or -NE shearing deformation [Faure et al., 1991; Gautier and Brun, 1994b, 1994a; Jolivet and Patriat, 1999; Mehl et al., 2005, 2007]. The central Cycladic detachment is associated to top-to-the-north deformation (Naxos, Paros) [Gautier et al., 1990; Buick, 1991; Gautier et al., 1993; Vanderhaeghe, 2004]. In all these islands, the detachment separates the lower metamorphic rocks from an upper plate, the upper Cycladic nappe, that has not recorded the Eocene HP metamorphism. In the

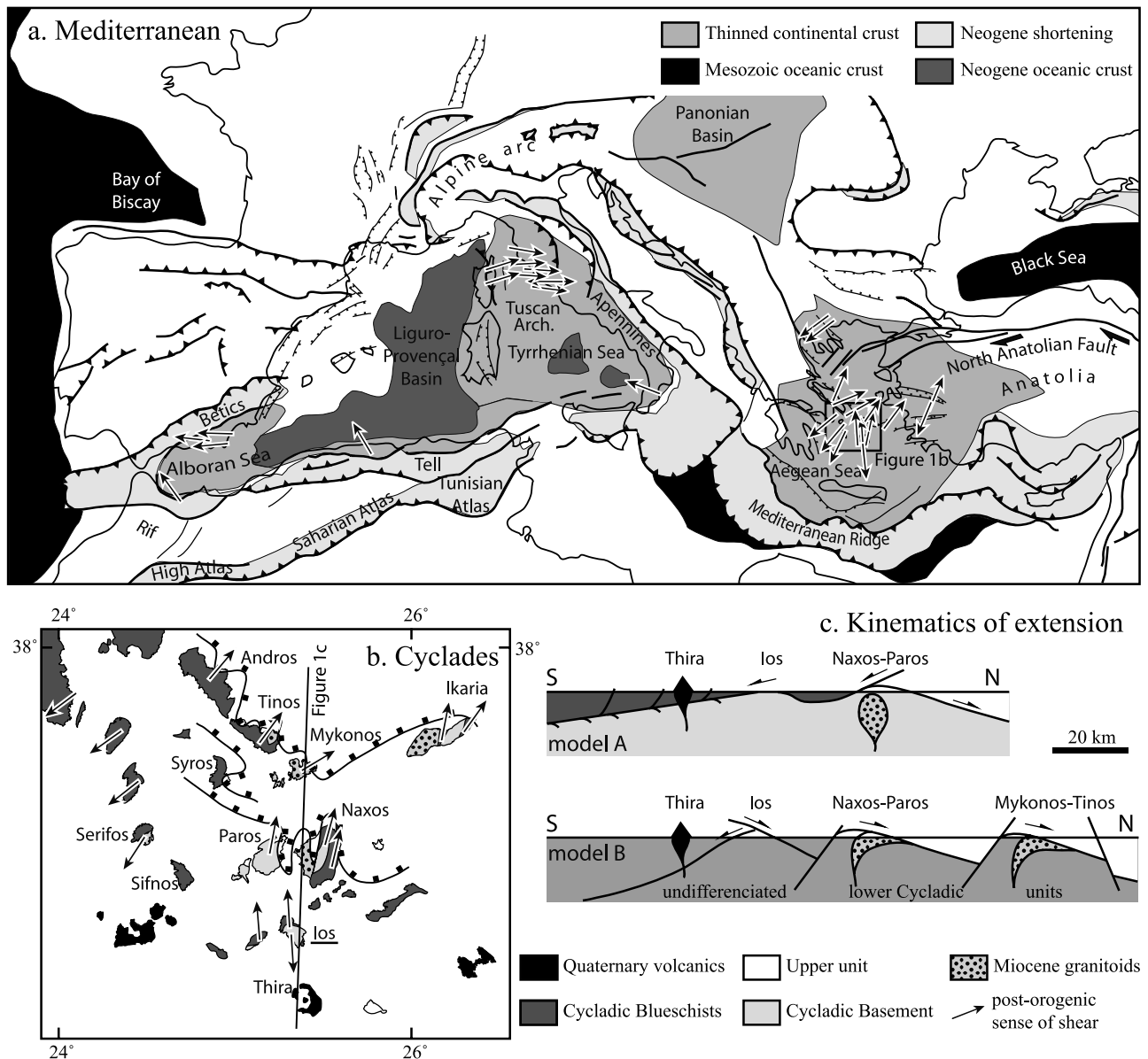


Figure 1

western Cyclades (Kea, Kithnos, Serifos), the observed sense of shear is top-to-the-southwest [Grasemann and Petrakakis, 2007]. The upper Cycladic nappe is not present on these latter islands and thus, strictly speaking, there is no detachment there but rather a brittle-ductile deformation with a top-to-the-southwest shear sense within the same unit. In the southern Cyclades, a complex extensional history with opposite top-to-the-north and top-to-the-south senses of shear has been described on Ios island [Lister et al., 1984; Vandenberg and Lister, 1996; Forster and Lister, 1999a]. Whether or not extension in the Aegean domain is symmetric or asymmetric depends on the regional importance given to the top-to-the-south senses of shear described on Ios and their relative chronology to the top-to-the-north movements (Figure 1c).

[7] In order to address these questions, we carried out a field study on Ios island. We aimed at (1) establishing a possible chronology between the top-to-the-north and the top-to-the-south structures and (2) understanding the role of each deformation event at regional scale. In this paper, we characterize the ductile deformation on Ios and we describe the chronological evidence and the relationships between deformation and metamorphism. Finally, we propose conclusions about the dynamics of the Cycladic domain during the synorogenic and postorogenic episodes.

3. Regional Geology and Tectonic Models

3.1. Geology of the Cycladic Archipelago

[8] Ios is one of the southernmost islands of the Cycladic Archipelago, located in the central part of the Aegean Sea (Figures 1a and 1b). These islands correspond to the internal part of the Hellenides-Taurides belt that was the result of the convergence between the Apulian and the European plates in the eastern Mediterranean [Aubouin and Dercourt, 1965; Brunn et al., 1976; Jacobshagen et al., 1978]. Classically, three main units are distinguished in the Cyclades [Bonneau, 1984, and references therein]: the lowermost Cycladic Continental Basement unit, the intermediate Cycladic Blueschists unit and the uppermost Pelagonian unit (upper Cycladic

nappe). The Cycladic Basement unit crops out on the central and the southern Cyclades (Naxos, Paros, Sikinos and Ios, Figure 1b) [Andriessen et al., 1987]. This unit is composed of granite, paragneiss and orthogneiss. Hercynian and pre-Hercynian ages as well as relict amphibolite facies assemblages suggest a complex prealpine history [Henjes-Kunst and Kreuzer, 1982; Andriessen et al., 1987]. The Cycladic Basement unit is considered to have been part of the Apulian southern margin of the Pindos basin [Bonneau and Kienast, 1982]. The Cycladic Blueschists unit is present on most Cycladic islands as an association of metapelites, marbles and metabasites. The metabasites are ancient flows, tuffs, or basic blocks in a mélangé as seen on Syros island [Bonneau et al., 1980]. Geochemistry indicates that they are mainly derived from MORB-type basalts [Schliestedt et al., 1987; Bröcker, 1990]. Two different paleogeographies have been proposed for the Cycladic Blueschists: either a Pindos affinity [Bonneau, 1982] or a Pelagonian affinity [Stampfli et al., 2003]. We use the Pindos basin origin as a working hypothesis. The Pelagonian unit appears as the upper unit on many Cycladic islands. It consists in ophiolitic material or high-temperature metamorphic rocks yielding late Cretaceous ages [Jansen, 1977; Dürr et al., 1978; Maluski et al., 1987; Patzak et al., 1994; Katzir et al., 1996].

[9] Two major tectonometamorphic episodes have been recognized in the Cyclades on the basis of structural, petrologic and radiometric studies: an Eocene episode of thickening during convergence followed by an Oligo-Miocene collapse associated to divergence. The sequence of burial and exhumation of the Cycladic Basement and Cycladic Blueschists units results from the succession of the two episodes. The first episode is associated to high-pressure–low-temperature (HP-LT) metamorphism under eclogite and blueschist facies conditions. It is largely documented in the Cycladic Blueschists but poorly recorded in the Cycladic Basement. Radiometric dating gives ages between 35 and 70 Ma in eclogite and blueschist facies rocks with limited retrogression [Bröcker et al., 2004, and references therein]. Most of them cluster between 40 and 50 Ma. The retrograde P-T paths of Syros and Sifnos [Trotet et al., 2001a, 2001b] and the first stage of the retrograde P-T paths of Tinos [Parra

Figure 1. (a) Tectonic map of the Mediterranean region showing the main mountain belts and regions of postorogenic extension as well as the Mesozoic and Cenozoic oceanic domains, modified after Jolivet et al. [2006]. The arrows indicate the ductile sense of shear associated to back-arc extension. (b) Tectonic map of postorogenic structures in the Cyclades, modified after Jolivet et al. [2004b]. The arrows indicate the ductile sense of shear associated to the Oligo-Miocene extensional episode [Lister et al., 1984; Faure et al., 1991; Gautier and Brun, 1994b; Vandenberg and Lister, 1996; Forster and Lister, 1999a; Jolivet and Patriat, 1999; Mehl et al., 2005, 2007; M. Müller et al., Extensional crustal-scale shear zones in the western Cyclades (Kea, Greece); paper presented at Symposium “Tektonik, Struktur und Kristallingeologie” 11, Göttingen, Germany, 2006; C. Rambahousek et al., The Serifos metamorphic core complex (Greece); kinematic investigations of the southern detachment mylonites, paper presented at Symposium “Tektonik, Struktur und Kristallingeologie” 11, Geowissenschaftliches Zentrum der Georg-August-Universität, Göttingen, Germany, 2006; K. Voit et al., Kinematics and deformation structures in a crustal-scale shear zone on Kea (W. Cyclades, Greece), paper presented at Symposium “Tektonik, Struktur und Kristallingeologie” 11, Geowissenschaftliches Zentrum der Georg-August-Universität, Göttingen, Germany, 2006]. (c) Published models for the Aegean back-arc extension. Model A shows that extension is dominated by top-to-the-south movements mainly expressed on Ios island [Lister et al., 1984; Vandenberg and Lister, 1996]. Model B shows that extension is accommodated by top-to-the-north and top-to-the-south structures; it is roughly symmetric [Forster and Lister, 1999a; Brichau, 2004]. The Cycladic Blueschists and Cycladic Basement units are not distinguished and are regrouped in a single metamorphic lower unit.

et al., 2002] and the southern part of Naxos [Martin, 2004] indicate that exhumation was active in HP-LT conditions in the subduction wedge. The Eocene HP-BT episode has been linked to the nappe stacking [Trotet *et al.*, 2001a]. However, the structures related to this episode are severely overprinted on most islands. It prevents from unraveling a clear kinematics for synorogenic exhumation at regional scale [Jolivet *et al.*, 2004b]. Nevertheless, coherent structures on Syros and Sifnos islands show that exhumation was accommodated by a continuous extension from ductile to brittle and from blueschist to greenschist facies conditions [Trotet *et al.*, 2001a, 2001b]. The associated sense of shear is top-to-the-east on Syros and top-to-the-northeast on Sifnos. On Syros, the contact between the upper Pelagonian unit and the lower Cycladic Blueschists unit appears as a synorogenic detachment [Trotet *et al.*, 2001a, 2001b]. It was active close to the subduction zone and participated in the early synsubduction exhumation of blueschists and eclogites. No synorogenic kinematics has yet been proposed for the contact between the Cycladic Blueschists and the Cycladic Basement units, in the Aegean.

[10] The second exhumation episode is associated to the retrogression of the HP-LT parageneses along a low-pressure–high-temperature (LP-HT) gradient in amphibolite and greenschist facies conditions that affected the three Cycladic units. Partial-melting conditions were reached in the Cycladic Basement on Naxos [Jansen, 1977]. Oligo-Miocene ages (15 and 25 Ma) have been obtained both for crystallization of crustal melts [Keay *et al.*, 2001; Martin *et al.*, 2006, 2008] and for partial annealing and cooling (with Rb/Sr, K/Ar and $^{40}\text{Ar}/^{39}\text{Ar}$ methods) [Wijbrans and McDougall, 1986; Andriessen, 1991; Bröcker and Franz, 1998; Duchêne *et al.*, 2006]. The LP-HT episode is associated to the intrusion of granitoid plutons dated from 9 to 19 Ma [Pe-Piper and Piper, 2002, and references therein]. This episode has been linked to the extension of the Aegean lithosphere in the back arc of the Hellenic subduction zone triggered at circa 25 Ma by the retreat of the African slab [Le Pichon and Angelier, 1981; Jolivet and Faccenna, 2000; Jolivet *et al.*, 2004a]. Extension led to the disruption of the nappe edifice and to the exhumation of the Cycladic Blueschists and the Cycladic Basement as the lower plate in MCCs separated from the Pelagonian upper unit by the postorogenic detachments mentioned above [Lister *et al.*, 1984; Avigad and Garfunkel, 1989, 1991; Gautier and Brun, 1994a; Avigad *et al.*, 1997; Jolivet *et al.*, 2004a].

3.2. Geology of Ios

[11] Ios appears as a dome structure cored by the lower Cycladic Basement and surrounded by the upper Cycladic Blueschists (Figure 2) [van der Maar, 1980; van der Maar and Jansen, 1983]. These papers provide a detailed description of the lithologies present on Ios.

[12] The Cycladic Basement unit is represented by a variably deformed Hercynian granite mantled by garnet micaschists. Metamorphosed mafic and pegmatitic intrusions are found in both lithologies. The hypothesis of an intrusive granite in a metasedimentary unit is favored [van der Maar,

1980; van der Maar and Jansen, 1983]. The prealpine history of the Cycladic Basement is documented by amphibolite facies parageneses in the garnet micaschist dated at 300 Ma [van der Maar, 1980; Henjes-Kunst and Kreuzer, 1982; Andriessen *et al.*, 1987; Baldwin and Lister, 1998]. HP-LT mineralogical indexes such as glaucophane, chloritoid, and jadeite in inclusions in albite and garnet [van der Maar, 1980; Henjes-Kunst and Kreuzer, 1982; van der Maar and Jansen, 1983] or clinopyroxene-garnet associations [Perraki and Mposkos, 2001] have been described. Peak conditions at 25 kbar and 540°C calculated with a phengite-garnet-omphacite paragenesis have been proposed [Perraki and Mposkos, 2001]. K-Ar and $^{40}\text{Ar}/^{39}\text{Ar}$ ages between 40 and 50 Ma were obtained for this episode [van der Maar and Jansen, 1983; Andriessen *et al.*, 1987; Baldwin, 1996; Baldwin and Lister, 1998]. Greenschist facies late chlorite-albite-biotite-garnet associations [van der Maar, 1980] with K-Ar and $^{40}\text{Ar}/^{39}\text{Ar}$ ages between 25 and 30 Ma [van der Maar and Jansen, 1983; Andriessen *et al.*, 1987; Baldwin and Lister, 1998] were correlated to the regional Oligo-Miocene LP-HT event. The Cycladic Blueschists unit is an association of marbles, metapelites and delaminated metabasites. Eclogitic and blueschist parageneses were preserved in metabasic pods embedded in a schist and marble matrix [Forster and Lister, 1999b]. The HP-LT event is characterized by the growth of glaucophane, omphacite, garnet and epidote [van der Maar, 1980; van der Maar and Jansen, 1983]. Retrograde blueschist facies assemblages overprinted the eclogite facies paragenesis during the very first steps of exhumation [Forster and Lister, 1999b]. Blueschist facies metamorphism is then retrograde; it is coeval with the first steps of exhumation. The peak conditions estimated for this episode are 9–11 kbar and 350–400°C [van der Maar and Jansen, 1983]. Isotopic dating provided ages between 40 and 50 Ma [van der Maar and Jansen, 1983; Baldwin, 1996]. The LP-HT event is characterized by the growth of secondary chlorite, albite and actinolite [van der Maar and Jansen, 1983] and is dated between 25 and 30 Ma [van der Maar and Jansen, 1983; Baldwin, 1996]. A third nonmetamorphic ophiolitic upper unit has also been distinguished in previous studies [van der Maar, 1980; van der Maar and Jansen, 1983]. It would be correlated to the Pelagonian upper unit of the other Cycladic islands. According to our observations, these rocks are the same greenschist and marble as those of the Cycladic Blueschists unit. Following Vandenberg and Lister [1996], we suggest that an upper unit does not exist on Ios.

[13] It must be emphasized that the conditions of the HP-LT event are poorly constrained. The estimation of 25 kbar and 540°C in the Cycladic Basement unit [Perraki and Mposkos, 2001] can be discussed. The 25% jadeite content in the clinopyroxene of the considered parageneses is too low to correspond to a proper omphacite [Meyre *et al.*, 1997]. This clinopyroxene does not belong to an eclogitic assemblage for the considered protolith chemistry. However, such clinopyroxenes are characteristic of LP-HT metamorphism in the amphibolite facies. We then argue that the clinopyroxenes considered by the authors are relicts of a prealpine episode and that the estimate cannot be considered as valid for the

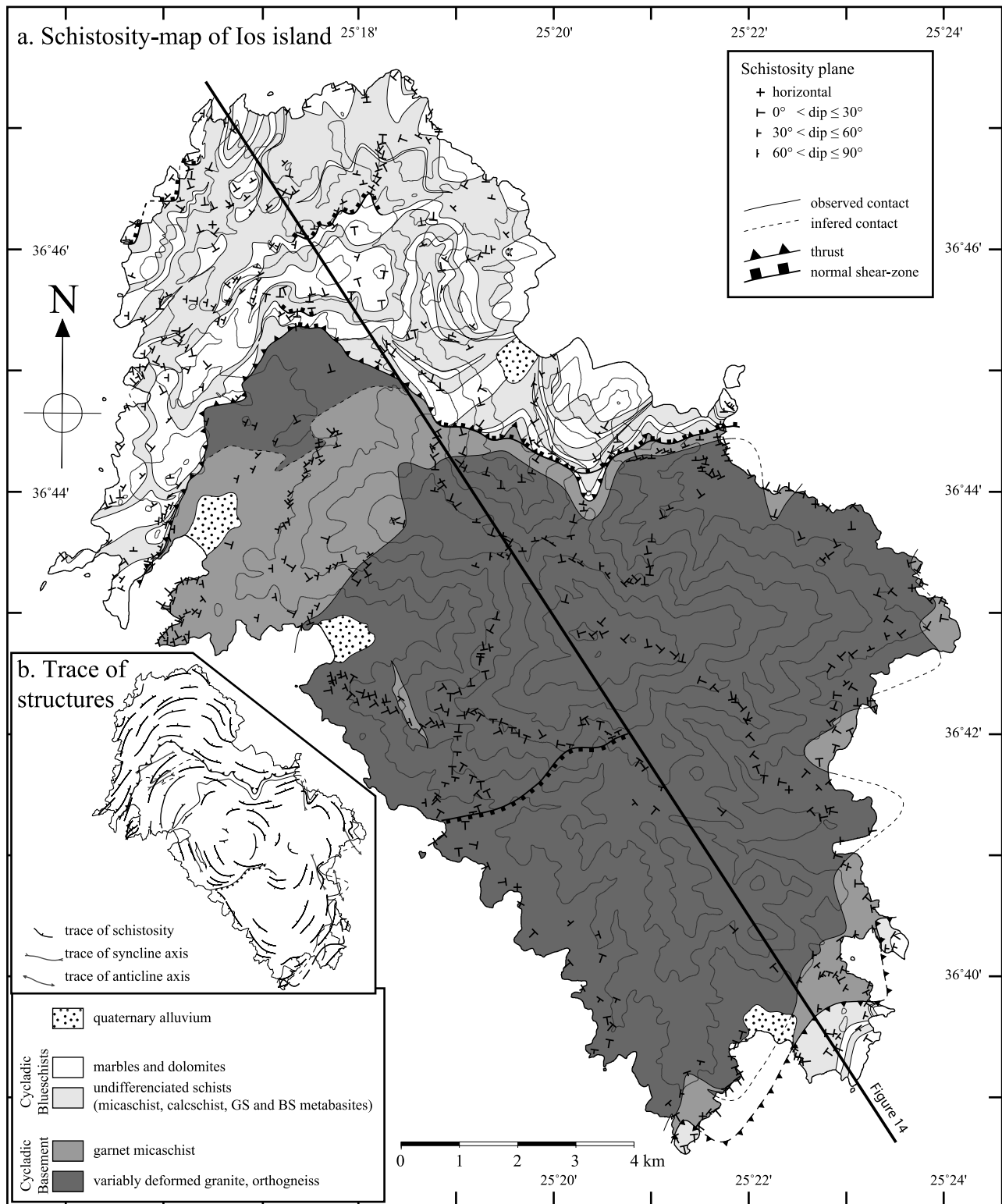


Figure 2. (a) Geological and schistosity map of Ios. The lithologic contours have been defined on the basis of our field observations. The measured values of dip and the major shear zones are indicated. (b) Simplified map of the schistosity trajectory and the main fold axes.

alpine HP-LT event. Besides, a recent estimate of the alpine pressure peak in the same unit on the neighboring island of Sikinos (Figure 1b) lies around 11 kbar and 475°C [Gupta and Bickle, 2004]. We consider this estimate as more accurate for the maximum conditions reached by the Cycladic Basement during the HP-LT episode. Furthermore, it has been argued that the maximum pressure reached in the Cycladic Blueschists unit may have been much higher than 11 kbar [Forster and Lister, 1999b]. This later value is not consistent with the eclogitic and blueschist facies parageneses already described in this unit [van der Maar and Jansen, 1983; Forster and Lister, 1999b]. Moreover, most recent petrologic studies on Tinos [Parra et al., 2002], Syros [Trotet et al., 2001a, 2001b], Sifnos [Trotet et al., 2001a, 2001b; Schmädicke and Will, 2003], Naxos [Martin, 2004], and Samos [Will et al., 1998] have calculated maximum pressures between 18 and 20 kbar for the HP-LT episode. Since the HP-LT parageneses described on Ios are the same as the ones described by these authors on other Cycladic islands, the range 18–20 kbar can be taken as an indicative estimate for the maximum pressure reached on Ios. It is therefore likely that maximum pressures reached by the Cycladic Blueschists unit are higher than the ones reached by the Cycladic Basement unit.

[14] We carried out field mapping in order to complement the Institute of Geology and Mineral Exploration map [van der Maar et al., 1981] (Figures 2–4). Two lithologies have been distinguished in the Cycladic Blueschists: schists (comprising micaschist, calcschist, eclogite, blueschist and greenschist facies metabasites) and marbles. In the Cycladic Basement, the garnet micaschist and the orthogneiss derived from the granite have been distinguished.

3.3. Previous Work

[15] Several tectonic models have been proposed for Ios island and particularly for the nature of the Cycladic Blueschists–Cycladic Basement contact. The first studies on Ios led to the suggestion that the contact between the two units is a thrust, active prior to or during the HP-LT event in synorogenic conditions [van der Maar, 1980; van der Maar and Jansen, 1983]. However, no kinematics was proposed for this thrust. The “synorogenic hypothesis” has been abandoned after the description of Ios as a MCC [Lister et al., 1984]. According to this latter study, the contact between the Cycladic Blueschists and the Cycladic Basement units is a crustal extensional shear zone associated to top-to-the-south movements that accommodated postorogenic extension. This contact is essentially expressed in the Cycladic Basement unit and has been named the South Cycladic Shear Zone (SCSZ) [Lister et al., 1984]. It has first been proposed that the SCSZ is the major extensional structure in the Cyclades and that it crosscuts the top-to-the-north detachment of Naxos-Paros [Vandenberg and Lister, 1996]. A later study details the tectonic evolution and distinguishes four successive families of extensional structures [Forster and Lister, 1999a]. (1) The top-to-the-south SCSZ is located in the upper part of the Cycladic Basement. (2) The Ios detachment system consists in anastomozed top-to-the-south

low-angle faults that truncate the SCSZ, and this structure allows the final juxtaposition of the two units. (3) Late top-to-the-north shear zones affect the SCSZ, but their significance remains enigmatic. (4) The Coastal fault array located in the northwestern coast only affects the Cycladic Blueschists unit, and it consists in shallow dipping anastomozed faults striking N–S to NE–SW. The top-to-the-west criteria overprint the top-to-the-north ones. In this study, the SCSZ, the Ios detachment system, the top-to-the-north shear zones, and the top-to-the-north faults of the coastal fault array are related to the regional north-south extension, and the top-to-the-north structures are arched during the later formation of the dome. Moreover, it is suggested that north-south extension began in blueschist conditions. Last, the results of a recent study of the late low-temperature evolution of Ios point out the importance of top-to-the-north asymmetric extension in the final part of the exhumation metamorphic rocks [Brichau, 2004].

[16] These different chronologic relationships between top-to-the-north and top-to-the-south movements have important consequences on the regional kinematics of the postorogenic extensional episode. Two models can be distinguished (Figure 1c). Model A favors the role of the SCSZ at regional scale [Lister et al., 1984; Vandenberg and Lister, 1996]. It leads to a top-to-the-south asymmetric model concerning the Aegean, with a minor top-to-the-north detachment. Model B considers successive top-to-the-south and top-to-the-north deformations on Ios [Forster and Lister, 1999a; Brichau, 2004]. In this model, the MCCs are exposed as horsts and postorogenic extension is fairly symmetric. It must be noted that no model is fully asymmetric, contrary to the other Mediterranean examples. The following describes the results of our field observations.

4. Finite Structure of Ios

4.1. Schistosity Defines a Structural Dome

[17] All metamorphic rocks of the Cycladic Blueschists, the garnet micaschists and part of the orthogneisses of the Cycladic Basement are pervasively foliated (see section 3.4 for a detailed analysis of strain pattern in orthogneiss). Primary compositional layering in the metasediments and metabasites of both units has been transposed into the schistosity. Recumbent tight to isoclinal folds observed at all scales are responsible for the transposition. Moreover, schistosity planes of different lithologies are generally concordant in the same unit. Across the Cycladic Blueschists–Cycladic Basement contact, schistosity planes have the same strike (Figures 2a and 2b). The dip of the schistosity is continuous through the contact in the southern part of the island, whereas it is not in the northern part.

[18] The dip of schistosity planes displays a large range of variation between 0° and 90° (648 measured schistosity planes, Figures 2a, 5a, and 5b). Eighty percent of dip values are between 10° and 50° and the mean dip value is about 30° (Figure 5b). Despite the dip dispersion, the schistosity planes commonly dip away from the center of the Island and the strike distribution shows a fairly concentric pattern. This

feature is best expressed in the northern part of the Cycladic Blueschists and near the coast (Figure 2b). The Cycladic Basement orthogneisses form the core of the domal structure whereas the upper Cycladic Blueschists lie in the outer part of the dome. This conclusion has already been reached in previous studies [van der Maar, 1980; van der Maar and Jansen, 1983; Vandenberg and Lister, 1996; Forster and Lister, 1999a].

4.2. Stretching Lineation Data and Fold Directions

[19] Stretching lineation is a common feature of metamorphic rocks of Ios island. It is defined by various markers depending on the nature of the protolith, the metamorphic grade and the intensity of strain. In marbles and dolomites, it is defined by very fine mica slates. In schists of both units (micaschists, calcschists, greenschist and blueschist), it is outlined by stretched quartz rods, by fibrous or slaty phyllosilicates growing in schistosity planes, by the elongation of prismatic minerals (glaucofan, epidote, albite) or by the direction of strain shadows. In orthogneisses, it is outlined by the elongation of primary minerals (K-feldspar and quartz) and by the growth of phyllosilicates in schistosity planes. The lineations considered as markers of finite deformation have been measured in the schistosity plane. On most outcrops, the orientation of various types of lineation is constant. 614 lineations have been measured throughout the island in all lithologies with metamorphic grade lower than blueschist (Figures 3a and 5c–5f). The strike of lineations in greenschist facies rocks shows low dispersion (Figures 5c and 5d). It is centered on an average value of N173 with 70% of the values found between N160 and N10 (Figure 5d). The statistical distribution of data and a computed Gaussian curve with the same average and standard deviation values have been compared. The peak showed by the data is even sharper than the one of the Gaussian curve. Considering the lineation in blueschist facies rocks, the average trend is also N173 (Figures 3a, 5e, and 5f). However, the strike distribution is more dispersed around the average value: the computed standard deviation reaches 36°. Only 30% of the values are between N160 and N010, whereas 61% of the values are between N150 and N020. This dispersion can be explained by two exclusive histories: (1) deformation in the blueschist facies was associated to a fairly N–S lineation, and the dispersion is synblueschist or due to postblueschist deformation; and (2) deformation in the blueschist facies was associated to a lineation that primarily did not strike N–S, and later deformation normalized the blueschist lineation to the N–S strike. Since no particular strike is emphasized by a frequency peak outside the N150–N020 band (Figure 5f), no remnant of a primary blueschist strike seems to exist. We then favor the first explanation. The plunge of lineation is generally shallow: it is lower than 30° in 73% of measurements (Figure 5c). This last feature is explained by the independence between the fairly constant strike of the lineation and the domal distribution of schistosity planes. Consequently, the stretching direction inferred from lineation strike is roughly N–S in the recorded ductile history of the Cycladic Blueschists and the Cycladic Basement.

[20] Two families of folds have been recognized. They are distinguished by the strike of their axis in comparison with the strike of the lineation. Tight to isoclinal recumbent and symmetric folds with axial plane parallel to the schistosity and axis collinear with the lineation transpose the primary compositional layering into the schistosity. These folds deform all lithologies of both units and are best expressed in marbles. Moreover, they can be observed at all scales from millimeter up to several kilometers (Figures 2a and 2b). Especially, by mapping the garnet-micaschists/orthogneiss contact, we found that it is deformed by kilometeric recumbent folds with axis parallel to the lineation. This kind of folds classically indicates a large component of simple shear as the axes have been rotated toward the shearing direction during progressive deformation. The second family corresponds to asymmetric south vergent folds. Their axial plane dips to the north, and their axis is roughly perpendicular to the lineation. These folds have been observed in the vicinity of the contact at small and large scales. The largest one is a south verging syncline of garnet-micaschist lying in the northern part of the Cycladic Basement (Figure 2a). The geometry and the kinematic interpretation of the second family of folds is detailed in section 5.

4.3. Strain Facies in the Orthogneiss

[21] Augengneisses are largely dominant in the orthogneiss of the Cycladic Basement unit. They are the result of the deformation of the same hercynian porphyroid granitic protolith that is preserved in the least deformed area [Vandenberg and Lister, 1996]. We can describe the pattern of deformation magnitude that affected the orthogneiss by mapping the state of finite deformation. Four strain facies of orthogneiss have then been distinguished (Figures 4b–4d and 6a–6d). They describe the intensity of deformation that affected the granitic protolith. Facies A corresponds to the undeformed protolith (Figures 4b and 6a). The fabric is equant, chlorite statically replaces biotite. Facies B corresponds to the lightly deformed protolith (Figures 4c and 6b). Deformation is localized along millimeter- to centimeter-thick shear bands. Primary minerals are reoriented: K-feldspar are aligned along the direction of the slickenslide on the shear bands, chloritized biotite is transposed into coarse planes that form a soft planar fabric. Very few minerals crystallize in the newly formed structures. Facies C corresponds to pervasively deformed augen gneiss (Figures 4d and 6c). K-feldspar and quartz are deformed: their flattening defines the schistosity and their elongation defines the lineation. No biotite is preserved. Phyllosilicate aggregates (chlorite and phengite) crystallize in the schistosity as slates parallel to the lineation. Facies D corresponds to a mylonitic orthogneiss (Figures 4e and 6d). The structures are the same as in facies C but K-feldspar and quartz are laminated and only a few porphyroclasts are preserved. From facies A to facies D, the average grain size diminishes and the proportion of phyllosilicate increases. This last observation may reflect the progressive strain-induced transformation of K-feldspar into phengite [Mitra, 1978; Gueydan et al., 2003]. At the island scale, the most strained rocks (facies C and D) lie in the vicinity of the top of the orthogneiss, under the

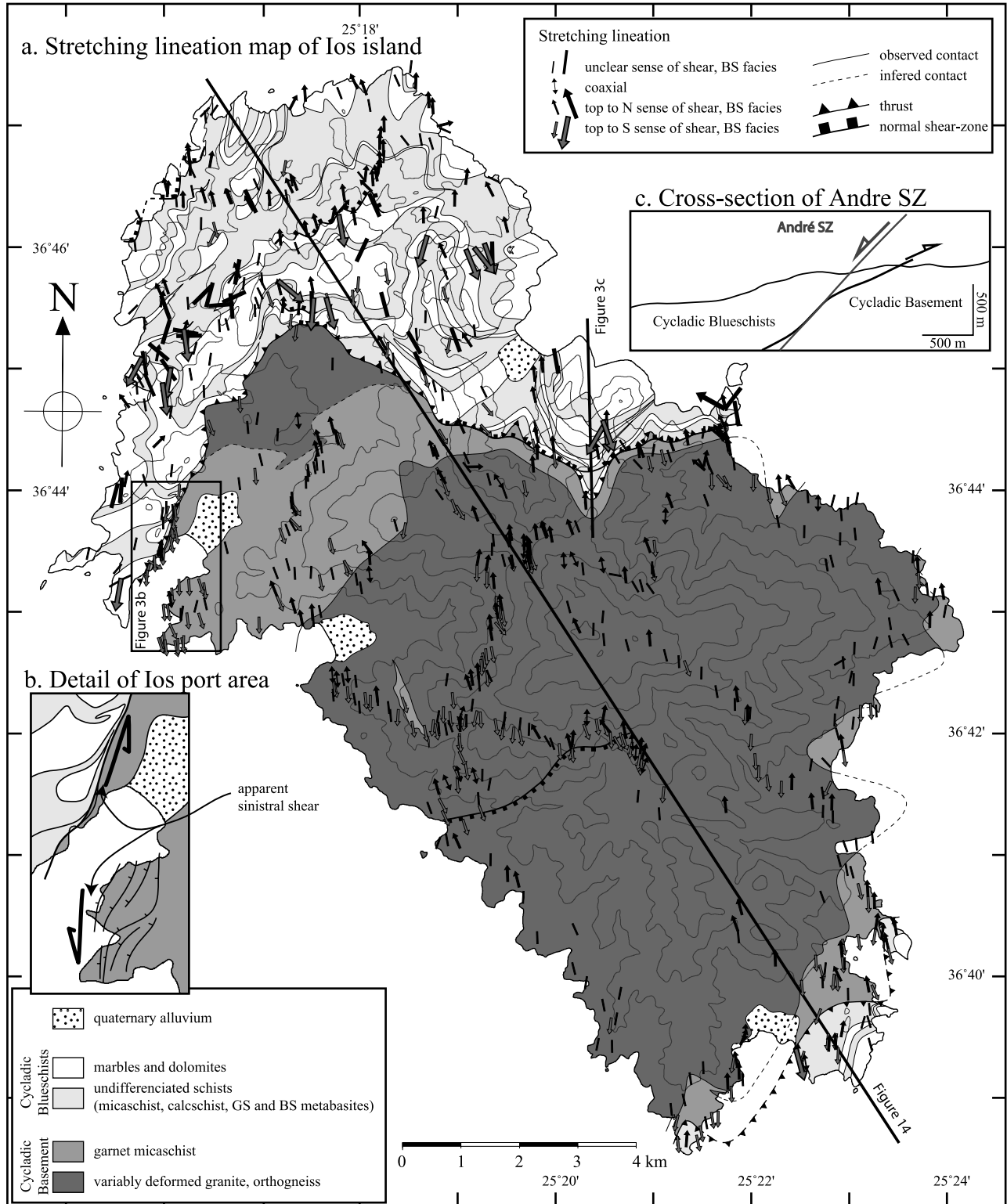


Figure 3. (a) Geological and stretching lineation map of Ios. The arrows indicate the sense of shear (top-to-the-north in black and top-to-the-south in gray). Lineations associated to blueschist facies assemblages (BS) are indicated by larger symbols. (b) Simplified cross section perpendicular to the André fault. The deformation of the Cycladic Blueschists–Cycladic Basement contact indicates the top-to-the-north sense of shear. (c) Detail of the map in the area of Ios harbor. The fold and the sigmoids indicate sinistral deformation consistent with top-to-the-south movements along the contact.

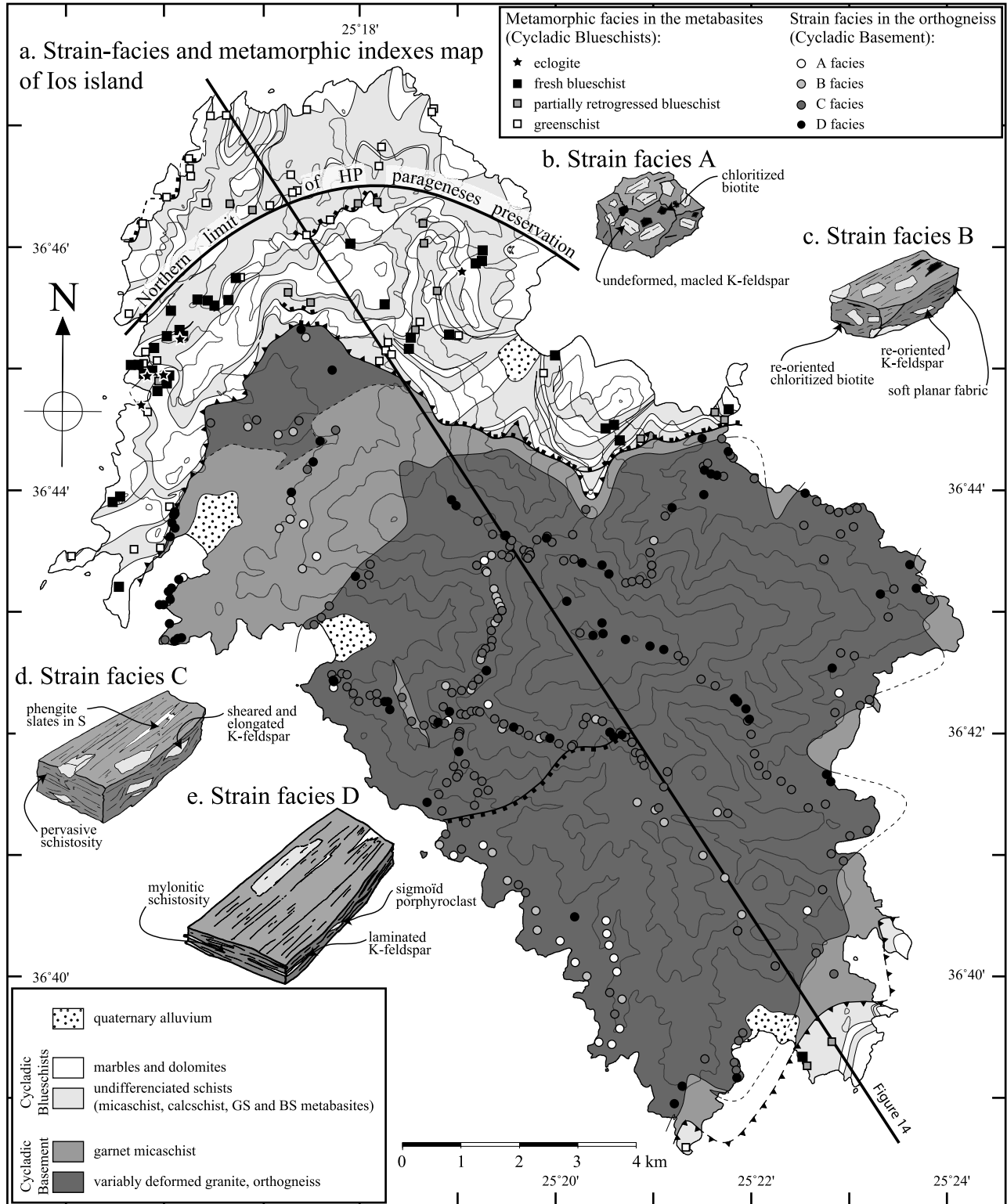


Figure 4. (a) Geological, strain facies, and metamorphic indexes map of Ios island. The metamorphic facies in metabasites of the Cycladic Blueschists unit is indicated: eclogites (star), fresh blueschist (black square), partially retrogressed blueschist (gray square), and greenschist (white square). Some of the eclogites occurrences are taken from other studies [van der Maar et al., 1981; Forster and Lister, 1999b]. Schematic diagrams for strain facies in the orthogneiss of the Cycladic Basement unit: (b) facies A, (c) facies B, (d) facies C, and (e) facies D.

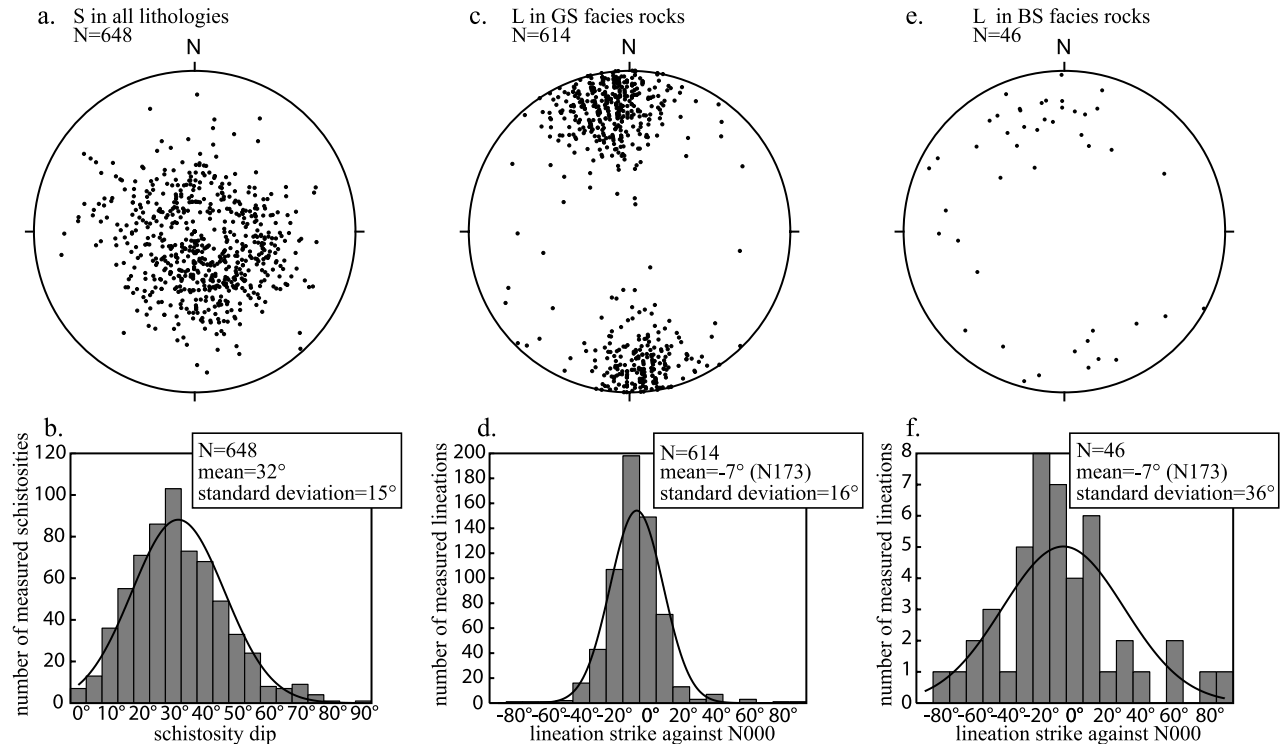


Figure 5. Schmidt's lower hemisphere equal-area projection of (a) schistosity poles, (c) lineations in greenschist facies rocks, and (e) lineations in blueschist facies rocks. Distribution frequency of (b) the schistosity dip, (d) lineations azimuth in greenschist facies rocks, and (f) lineations azimuth in blueschist facies rocks. Comparisons with Gaussian distributions are displayed (black curve).

garnet micaschist or the Cycladic Blueschists (Figure 4a). They crop out on the summit of the island and on nearby ridges. The uppermost part of the orthogneiss is frequently marked by a meter-to-decameter thick band of mylonites made of facies D gneiss grading into facies C. This carapace lies above the less strained rocks (facies A and B) that crop out in the core of the dome and in the southern part of the orthogneiss (Figure 4a). Facies B rocks are dominant and make the transition between the carapace and the undeformed granite. However, it must be emphasized that the thickness of the carapace is highly variable. Pervasive strain is generally distributed through ~ 100 –800 m, whereas it is distributed through 5 m only in the southwestern part of the orthogneiss. The distribution of strain facies in the orthogneiss highlights a kilometric strain gradient: finite deformation increases from the lowest part to the upper part of the orthogneiss. Strain gradients have also been observed at decameter scale. In large strain areas of facies C or D, undeformed protolith of facies A can be preserved in lenses surrounded by B facies gneiss. In these cases, the schistosity and the lineations are concordant for all strain facies. This illustrates the heterogeneity of deformation at mesoscale [Vandenberg and Lister, 1996]. The presence of the carapace of more deformed orthogneiss shows that the Cycladic Basement has been sheared at the contact with the Cycladic Blueschists. The overall pattern of finite deformation is consistent with the Alpine dome structure. We therefore assume that most of it was acquired during

the Alpine episode. If present, hercynian heritage has been transposed into alpine orientations.

5. Kinematics of Deformation in the Cycladic Blueschists–Cycladic Basement Contact

5.1. Evidence of Top-to-the-South Movements in the Contact

[22] Generally, rocks in the direct vicinity of the Cycladic Blueschists–Cycladic Basement contact exhibit top-to-the-south shearing deformation (Figure 3a). The Cycladic Blueschists–Cycladic Basement contact is well exposed on the coast, west of Ios harbor (Figure 3c). In this outcrop, the schistosity and the contact strike NNE–SSW and dip gently to the NW. All lithologies experienced top-to-the-south shearing deformation. Several continuous cross sections can be observed on the coast. They are summarized on a 3-D diagram (Figure 7). The lower levels of the Cycladic Blueschists unit are composed of schist-marble breccia alternations. The thickness of the breccias is between 1 and 10 m. The size of clasts is between 5 and 50 cm. They are embedded in red cement that we supposed to be composed of carbonates. The schist levels are severely mylonitized and deformed by pervasive top-to-the-south shear bands. The lowest level of the Cycladic Blueschists unit is a 50 cm thick, highly laminated marble level. The garnet-micaschists of the

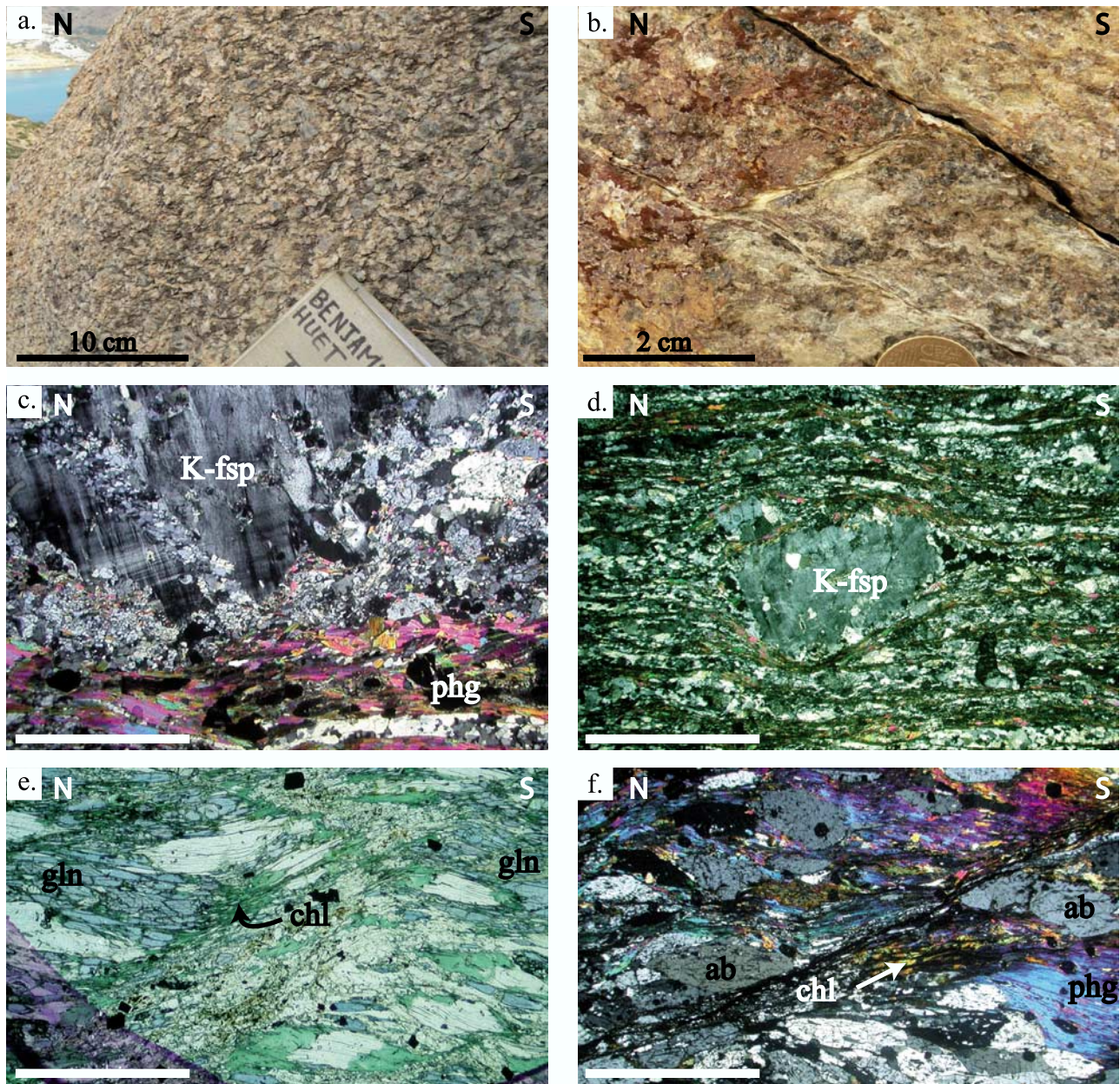


Figure 6. (a) Facies A granite. (b) Facies B orthogneiss. Deformation took place along thin anastomosed shear bands. (c) Facies C orthogneiss. The large K-feldspar porphyroclast suffered fracturation and recrystallization in the small bands. Phengite crystallized in the shear band below the porphyroclast. (d) Facies D orthogneiss. The small K-feldspar porphyroclast is surrounded by a quartz-phengite-chlorite matrix. (e) Top-to-the-north shear band in a glaucophane schist from the Cycladic Blueschists. The glaucophane is retrogressed into chlorite in and around the shear band. (f) Typical chlorite-phengite-albite greenschist facies association in the schists of the Cycladic Blueschists. The minerals are synkinematic. In Figures 6c–6f, the scale bar corresponds to 0.5 mm. K-fsp, K-feldspar; phg, phengite; gln, glaucophane; chl, chlorite; ab, albite.

Cycladic Basement unit are also severely deformed. Top-to-the-south shear bands are found everywhere; they are pervasive. Systematic folds with axes parallel to the lineation transpose the schistosity. They signal that the upper part of the Cycladic Basement experienced important flattening and shearing. Quartz lenses are also folded and transposed in the

schistosity. They are big and numerous compared to the rest of the Cycladic Basement unit. This observation can be an evidence of important fluid circulations. Large-scale structures around the Cycladic Blueschists–Cycladic Basement contact indicate the same southward movement. The shape of the marble levels lying just above the contact exhibits

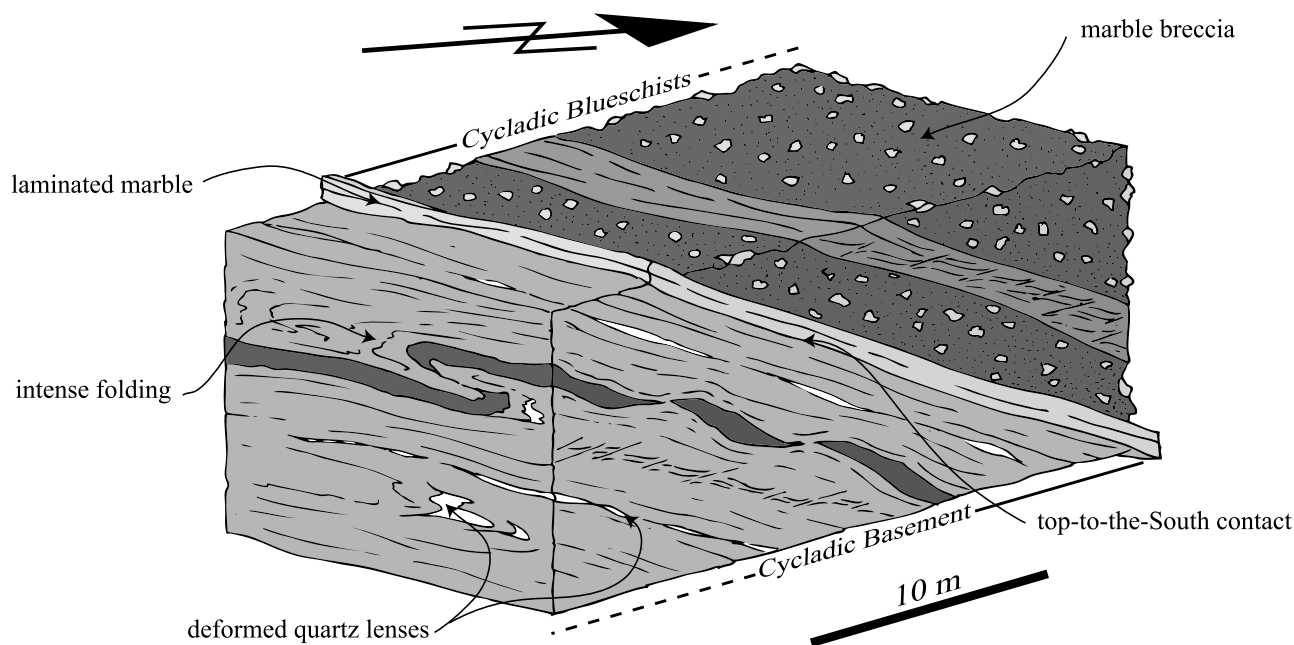


Figure 7. Synthetic 3-D diagram of the deformation associated to the Cycladic Blueschists–Cycladic Basement contact in Ios harbor area. The shear criteria indicate top-to-the-south sense of shear.

particular patterns (Figure 3b). The northern level is affected by asymmetric folding and the southern one gets thinner toward the north. Both structures show sinistral deformation. Below the contact, the schistosity of the garnet micaschist exhibits a kilometric sinistral sigmoid. The apparent sinistral deformation in both units in places where the schistosity dips to the W–NW is consistent with top-to-the-south deformation. The Cycladic Blueschists–Cycladic Basement contact and the juxtaposition of the two units are related to top-to-the-south movements.

5.2. Evidence of Top-to-the-North Extensional Overprint in the Contact

[23] Extensional deformation dominated by top-to-the-north asymmetry has also been observed in the contact. In the northernmost part of the Cycladic Basement unit, the contact separates micaschists of the Cycladic Blueschists and mylonitic orthogneisses of the Cycladic Basement (Figure 8). The contact is materialized by a two meter thick extensional shear zone composed of multiple normal faults in brecciated orthogneiss. In the footwall, extension is accommodated by north dipping normal faults, whereas in the hanging wall, south dipping faults dominate. This pattern indicates strain partitioning in the two blocks. Within the shear zone, a few small tilted blocks are preserved from brecciation (Figure 8b). In these blocks, earlier structures are preserved. The mylonitic schistosity is associated to penetrative S–C' structures indicating top-to-the-south shearing deformation.

[24] Mapping of the contact provided more evidence of top-to-the-north overprint. In the western part of Ios, the map indicates that the contact is not a planar structure (Figure 3a). It is in fact deformed by a large north dipping shear zone (Figure 3c). This structure has already been recognized and

named the Andre fault [van der Maar, 1980; van der Maar and Jansen, 1983]. The sigmoidal shape of the contact indicates top-to-the-north movements along the Andre fault (Figures 3a and 3c). It must be noted that the normal top-to-the-north shear zone does not reactivate the contact but rather deforms it as a passive marker.

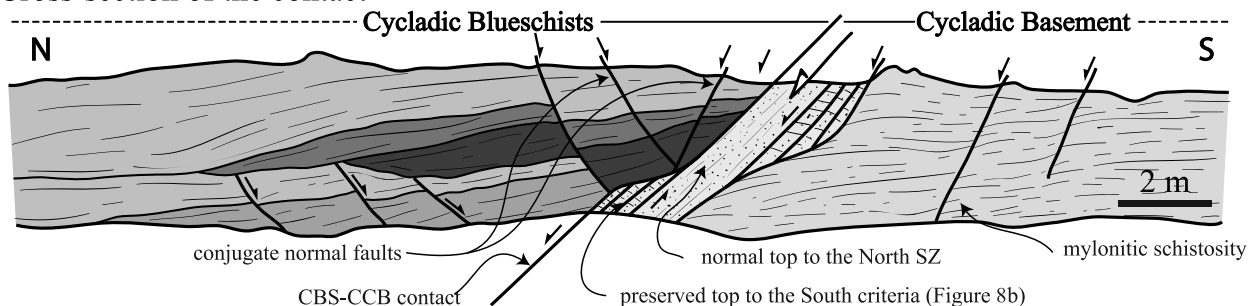
6. Characterization of the Top-to-the-South Deformation

6.1. Evidence and Distribution of the Top-to-the-South Deformation in the Cycladic Blueschists Unit

[25] Kinematics indicators of top-to-the-south deformation are very common, varied and often straightforward in the Cycladic Blueschists. In this unit, top-to-the-south deformation is characterized by pervasive structures affecting all lithologies at various scales.

[26] All kinds of schists (calcschist, micaschist, greenschist and blueschist facies metabasites) are affected by top-to-the-south shear bands (Figures 9 and 11a). The shear band spacing ranges from a few millimeters to a few centimeters in the weakest levels and from a few centimeters to a few decimeters in the most competent levels. The angle between the shear bands and the schistosity varies from 25° to 55°. It is highly variable within the same outcrop as well. On most outcrops, shear bands have an apparent normal offset. However, a few reverse shear bands have been observed in the vicinity of the Cycladic Blueschists–Cycladic Basement contact. Competent levels embedded in a weak matrix experienced boudinage with a southward asymmetry (Figure 9b). Eclogites and blueschists appear as decimetric to decametric asymmetric pods separated by top-to-the-south shear bands

a. Cross-section of the contact



b. Detail of top to the South preserved S-C' structures

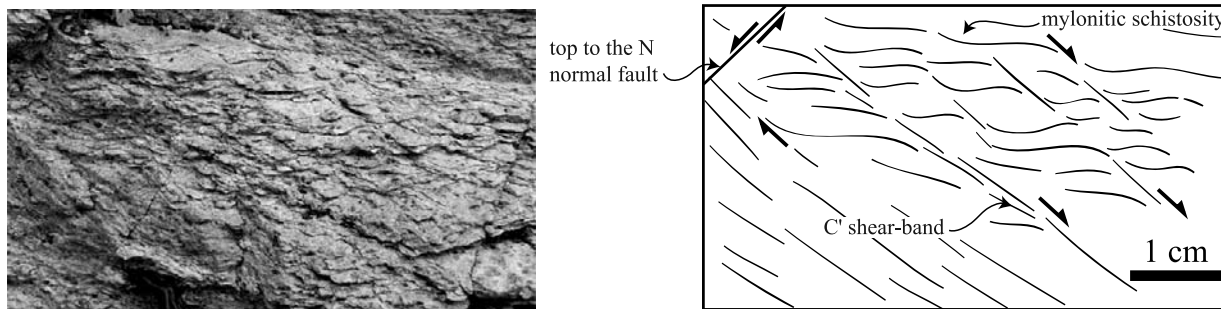


Figure 8. (a) Cross section of the Cycladic Blueschists–Cycladic Basement contact. The contact appears as a normal top-to-the-north shear zone. (b) Photograph of top-to-the-south structures preserved in the shear zone.

in the micaschist matrix. Moreover, within marbles, the dolomitic levels experienced book shelf faulting with deflection of markers compatible with a top-to-the-south sense of shear [Grasemann *et al.*, 2005]. At smaller scale, the garnet porphyroclasts of blueschist facies rocks are very often surrounded by asymmetric strain shadows also compatible with a top-to-the-south sense of shear (Figure 9c).

[27] A few decimetric south verging asymmetric folds have been observed in the vicinity of the Cycladic Blueschists–Cycladic Basement contact. Besides, in the western flank of the dome where the schistosity dips toward the west, we mapped decimetric asymmetric folds shaped by the marble levels. Their axes are roughly perpendicular to the N–S direction, and they are also south verging. The asymmetry of folds is compatible with a top-to-the-south sense of shear [Passchier and Trouw, 2005]. It must be noted that no real crenulation cleavage is associated to these folds. Top-to-the-south deformation has then been accommodated by the formation of shear bands rather than by south vergence asymmetric folding.

[28] A clear trend appears in the structural distribution of top-to-the-south kinematics indicators (Figure 4a). On the one hand, they are distributed throughout the south of the island. On the other hand, in the north of the island, they define a ~2 km thick level above the Cycladic Blueschists–Cycladic Basement contact. Its top is roughly concordant with the schistosity. Within this level, we have never observed top-to-the-south deformation localizing on large-scale structures. Even if top-to-the-south deformation is homoge-

neous, it tends to intensify in the vicinity of the Cycladic Blueschists–Cycladic Basement contact and to localize in the contact.

6.2. Evidence and Distribution of the Top-to-the-South Deformation in the Cycladic Basement Units

[29] The garnet-micaschists and the orthogneiss of the Cycladic Basement have recorded top-to-the-south deformation in very different manners. Rocks overlying the garnet-micaschists are as intensely schistosed as the Cycladic Blueschists schists and they seem to have approximately the same mechanical properties. Yet, three interesting large-scale features must be emphasized. First, in the southernmost part of Ios, we observed a succession of large top-to-the-south shear bands roughly parallel to the Cycladic Blueschists–Cycladic Basement contact. The associated sigmoids are about 50 m long and the schistosity in their cores is flat. Second, in the northwestern part of the garnet-micaschists, the trace of the schistosity points out a kilometric sinistral sigmoid (Figures 2b and 3b) compatible with a top-to-the-south sense of shear. Third, the garnet-micaschist appears in synformal position in the northern part of the Cycladic Basement unit. This kilometric fold has an asymmetry also compatible with a top-to-the-south sense of shear. In the Cycladic Basement orthogneiss, the top-to-the-south deformation is heterogeneous (Figure 4a). Least deformed rocks show millimeter thick shear bands. The deformation of a discrete schistosity indicates top-to-the-south deformation. These structures correspond to facies A (Figure 4b). With increasing strain,

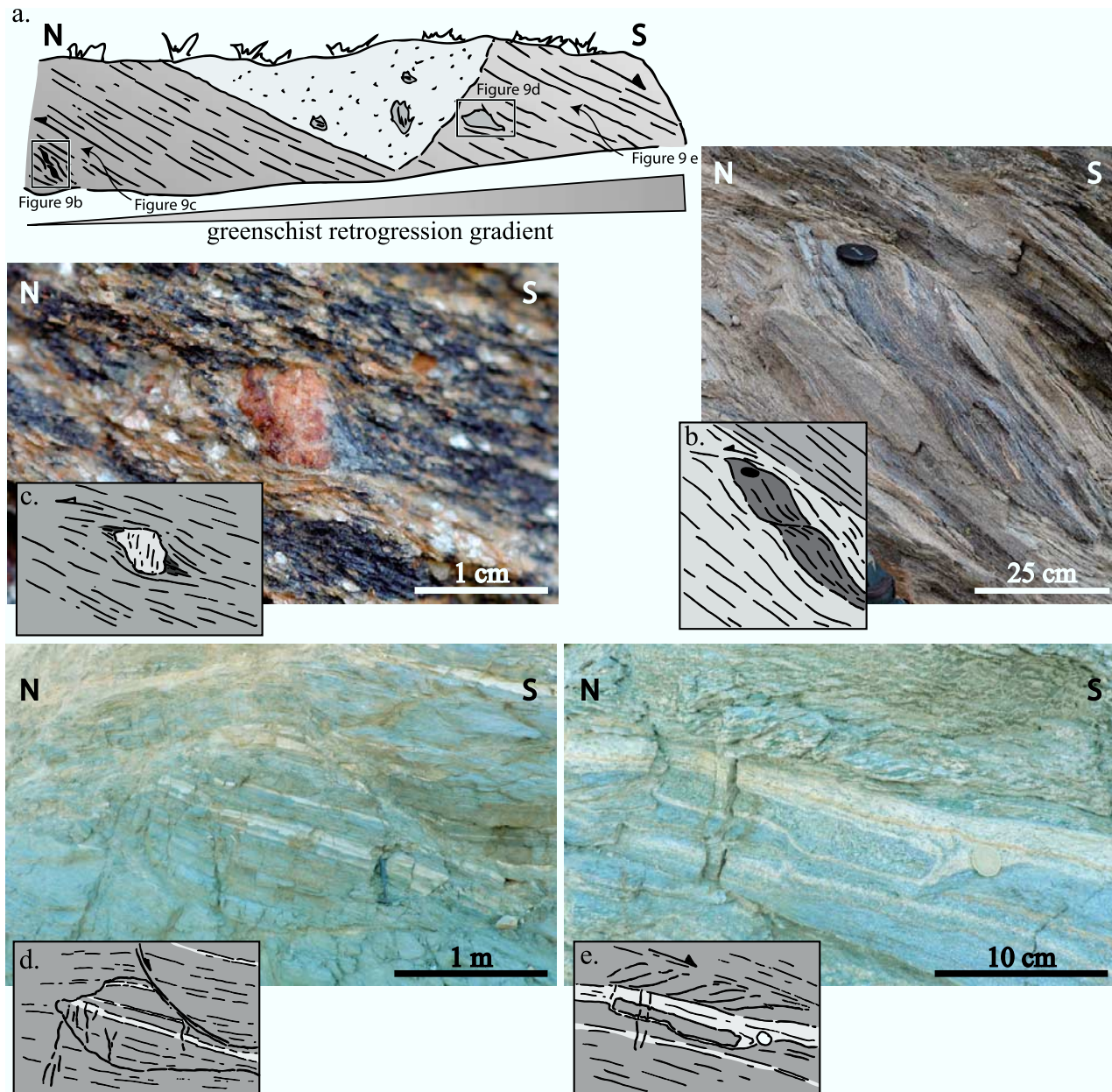


Figure 9. Deformation and metamorphic facies in the Cycladic Blueschists. (a) Diagram of an outcrop showing blueschist facies top-to-the-south structures (Figures 9b and 9c) in the south and greenschist facies top-to-the-north structures (Figures 9d and 9e) in the north. (b) Top-to-the-south asymmetric boudinage affecting a blueschist facies metabasic lens. (c) Top-to-the-south glaucophane pressure-shadow around a garnet. (d) Boudinage of greenschist with a top-to-the-north normal shear band rooting in the schistosity. (e) Top-to-the-north shear band in greenschist facies rocks.

anastomosed shear bands develop (Figure 10). The network consists in two kinds of shear bands. The dip of the longest ones is quite steady whereas the dip of the shortest is variable. The thickness of the longest ones (3–5 cm) is also greater than the thickness of the shortest ones (~1 cm, Figure 10b). Moreover, the longest shear bands are placed at regular interval of 2–3 m. These complex networks are completed by antithetic steep top-to-the-north shear bands (Figure 10). These structures correspond to the facies B (Figure 4c). S–C'

structures are typical structures of the augengneiss deformed by top-to-the-south deformation (Figure 10c). The spacing of C' bands is controlled by the size of K-feldspar porphyroclasts. The most strongly flattened porphyroclasts also experienced asymmetric folding consistent with the sense of shear. The S–C' structures are found in rocks of facies C (Figure 4d). Last, in the mylonites (facies D, Figure 4e), the asymmetry of porphyroclasts indicates that the mylonites were formed by top-to-the-south deformation. Except for

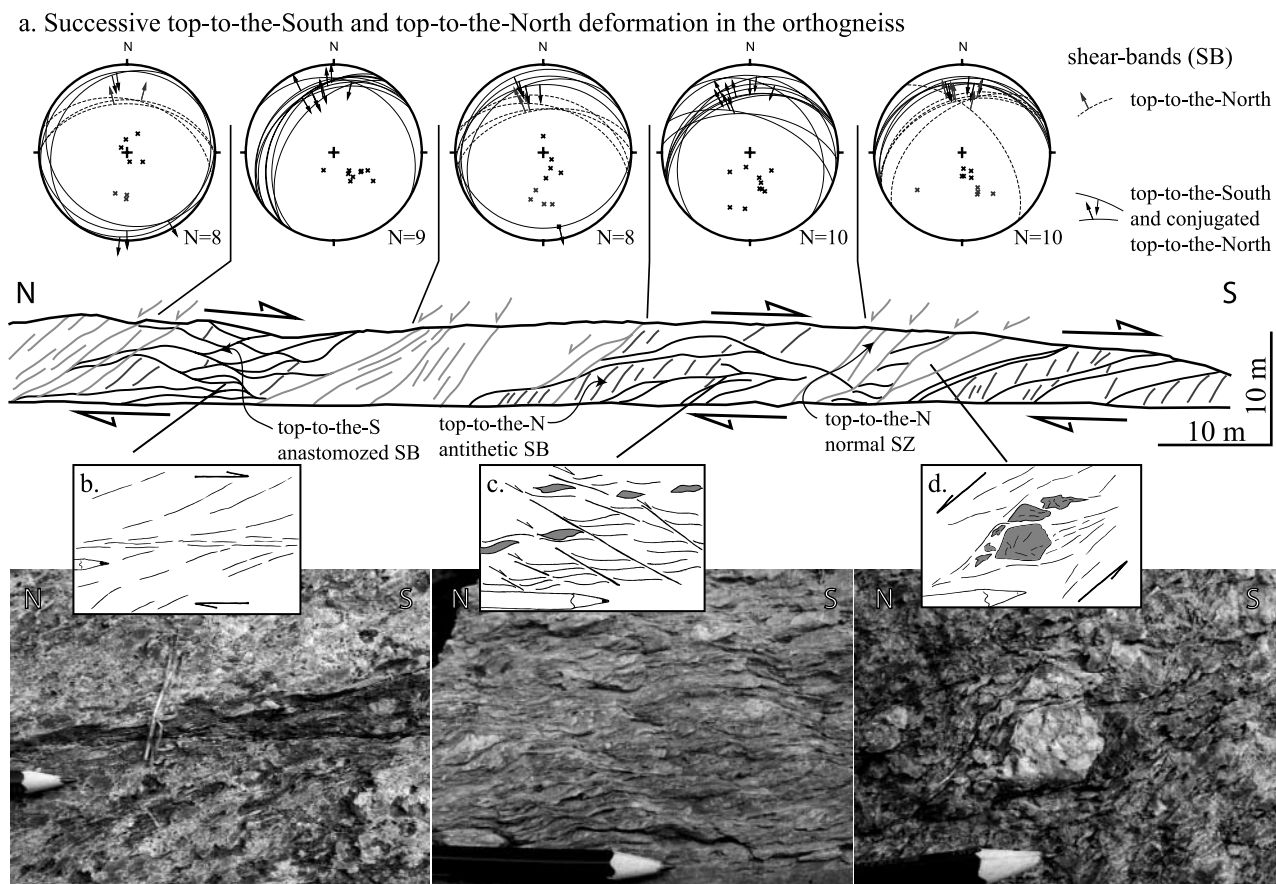


Figure 10. Deformation in the orthogneiss of the Cycladic Basement. (a) Two successive episodes of deformation can be recognized: top-to-the-south deformation is expressed by anastomosed shear bands associated to antithetic top-to-the-north shear bands and followed by top-to-the-north extensional shear zones. The Schmidt's lower hemisphere equal-area projections of the three types of shear bands are indicated. (b) Detail of a top-to-the-south shear band. (c) Top-to-the-south C' shear bands in a highly deformed zone between closely spaced shear bands. (d) Fracturing of K-feldspar in a top-to-the-north shear zone.

two locations, the schistosity of top-to-the-south mylonites is concordant with the pervasive schistosity of facies C orthogneiss. The two exceptions are located in the southern part of the island. In these cases, the mylonites are associated to steeply deepening shear bands (60°) that crosscut the regional schistosity. We believe that these structures are late and that they are not related to those described above.

[30] Variations in the intensity of the top-to-the-south deformation are responsible for the heterogeneity of finite deformation in the Cycladic Basement orthogneiss. As already pointed out (section 3), the structural distribution of finite strain facies defines a vertical strain gradient. As a result, the vertical strain gradient is a consequence of top-to-the-south deformation. The upper part of the orthogneiss has accommodated more finite deformation associated to top-to-the-south displacements than the lower parts.

6.3. Metamorphic Conditions of the Top-to-the-South Deformation

[31] The growth of synkinematic minerals is a good indicator of the physical conditions of the deformation. In

order to determine metamorphic conditions of the top-to-the-south deformation, we examined (when possible) the minerals that crystallized in shear bands and in associated strain shadows.

[32] The parageneses in metabasic rocks are a straightforward indicator of P-T conditions recorded by the rocks. In the Cycladic Blueschists, we distinguished four kinds of associations: eclogites, fresh blueschists, partially retrogressed blueschists and greenschists (Figure 4). Preserved HP-LT parageneses are located in the same structural level as top-to-the-south indicators. This observation points out a strong correlation between the preservation of HP-LT metamorphism and the presence of top-to-the-south deformation structures at large scale. The same correlation has been observed at the outcrop scale. Indeed, HP-LT metamorphic rocks that did not experience retrogression often show pervasive top-to-the-south deformation (Figures 9a–9c and 11a). We have furthermore observed glaucophane filling top-to-the-south strain shadows around garnets (Figure 9c). The glaucophane attests that the top-to-the-south rotational

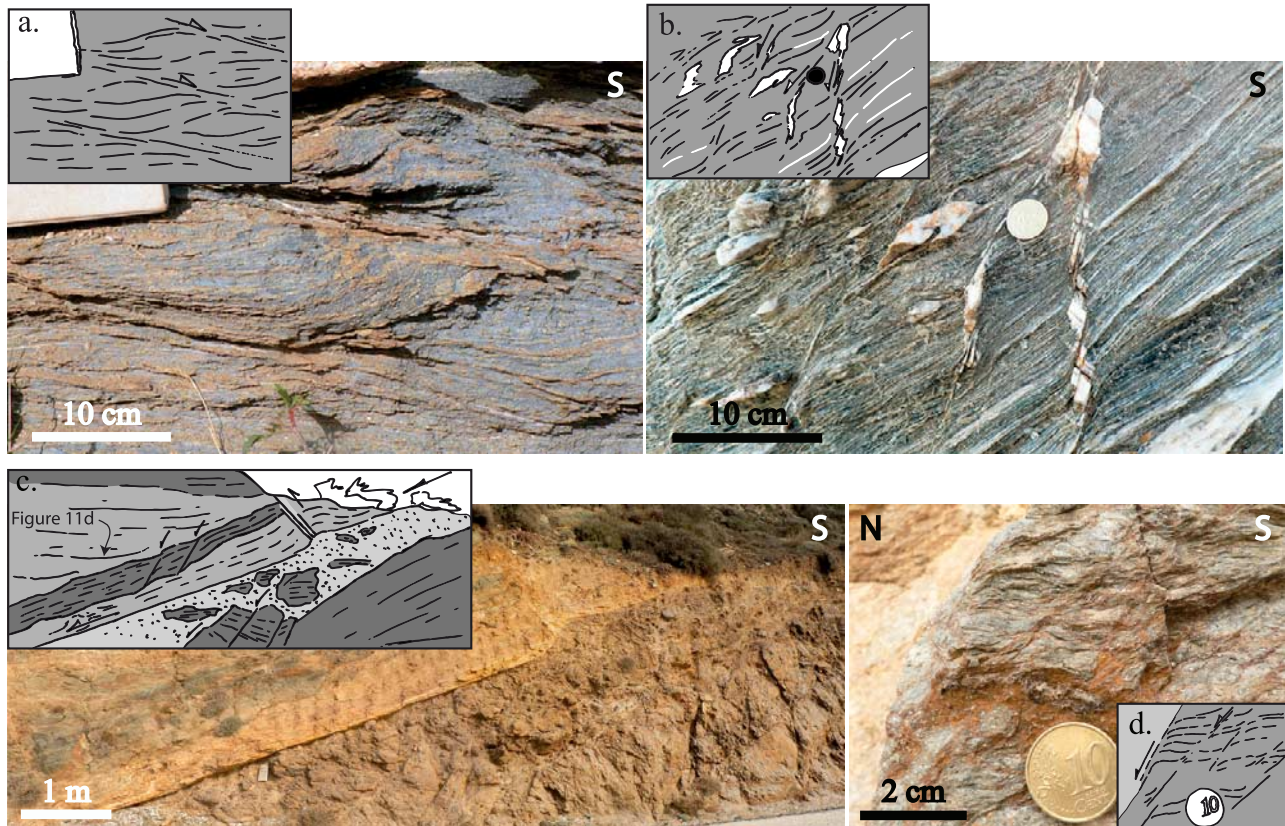


Figure 11. (a) Top-to-the-south shear bands in epidote-blueschist metabasites. Glaucophane and epidote grow in the shear bands. (b) C' -type cleavage with top-to-the-north movements. Quartz veins crystallized in the shear bands. They have pull-apart shape. (c) Top-to-the-north shear bands parallel to the schistosity. They induced brecciation in the schists. (d) Top-to-the-north C' -type cleavage in chlorite schist. Detail of the outcrop shown on Figure 11c.

deformation has partly acted in HP-LT conditions. Top-to-the-south shear bands filled by glaucophane and epidote (Figure 9f) lead to the same conclusion. The criteria of syn-HP-LT conditions top-to-the-south deformation are reported by large southward arrows on Figure 3a. Top-to-the-south structures coeval with greenschist facies conditions must also be taken into account. In greenschist facies metabasites, in micaschists and in calcschists, top-to-the-south deformation is associated to chlorite and phengite.

[33] In the Cycladic Basement garnet-micaschists, helicitic Mn-rich garnets are very common. Their shape is compatible with a top-to-the-south sense of shear. These synkinematic garnets are surrounded by strain shadows filled by phengite, chlorite and/or biotite. A few metabasic pods sheared southward appear in the garnet-micaschists. They show either prealpine amphibolitic parageneses strongly retrogressed into chlorite and phengite, or blue-green amphibole associated to epidote. These minerals attest epidote-amphibolite facies conditions. In the orthogneiss, the only minerals growing in top-to-the-south shear bands are chlorite and phengite. As a result, top-to-the-south deforma-

tion is at most associated to epidote-amphibolite facies conditions.

7. Characterization of the Top-to-the-North Deformation

7.1. Evidence and Distribution of Top-to-the-North Deformation in the Cycladic Blueschists

[34] In the Cycladic Blueschists, the most common ductile indicator of the top-to-the-north kinematics is the C' -type cleavage [Passchier and Trouw, 2005]. The spacing between the shear planes varies between a few millimeters up to 10 cm (Figures 11b and 11d). The C' -type cleavage exhibits particular characteristics. The shear planes are associated to a drastic reduction of the grain size: the average grain size of the minerals in schistosity is millimetric whereas it is about $10 \mu\text{m}$ in the shear planes. The angle between the schistosity and the shear plane is most often greater than 45° ; it could even reach 80° (Figures 9e, 11b, and 11d). These features could be interpreted by a component of brittle mechanisms during the top-to-the-north deformation. Between the shear

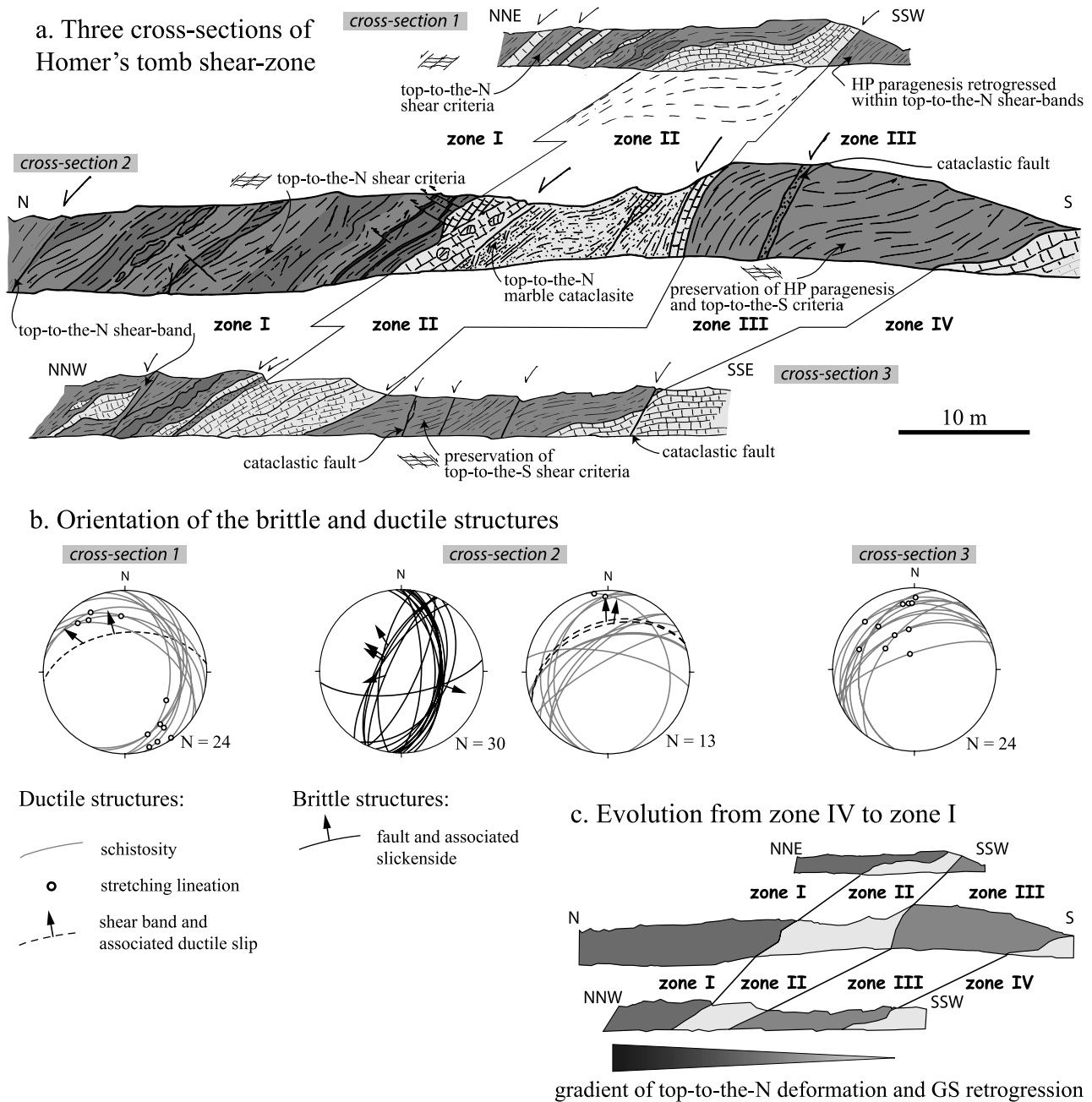


Figure 12. (a) Three cross sections perpendicular to Homer's tomb top-to-the-north extensional shear zone. Top-to-the-south shear criteria are preserved in the footwall of the shear zone. Top-to-the-north deformation dominates. (b) Schmidt's lower hemisphere equal-area projections of ductile and brittle structure. The direction of extension exhibits a deviation between the ductile and the brittle structures. (c) The evolution from zone IV to zone I (see text) defines a gradient of top-to-the-north deformation and greenschist retrogression.

planes, the strain shadows around albite, garnet, or epidote are asymmetric and indicate the same top-to-the-north sense of shear. Asymmetric boudinage of competent layers has also been observed. The shear planes separating the boudins frequently root in the schistosity (Figure 9d).

[35] Top-to-the-north shear zones parallel to the schistosity have been observed (Figures 11c, 12, and 13). They are filled by heterometric cataclastic breccia. Their kinematics is indicated by the shear bands and the faults affecting the breccia. The thickness of the shear zones is generally lower

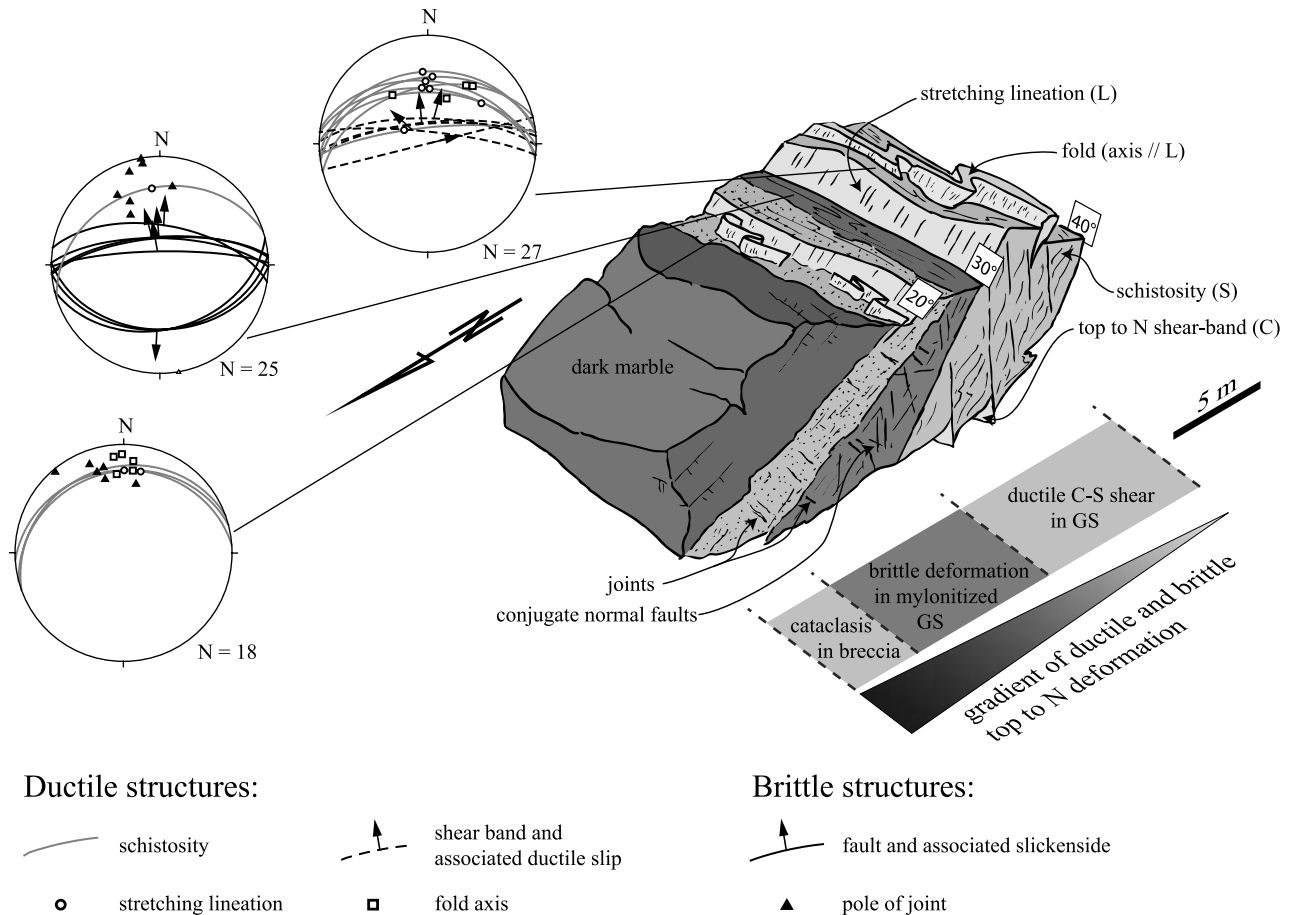


Figure 13. Schematic 3-D diagram of the Kambaki top-to-the-north extensional shear zone. The top-to-the-north deformation evolves from ductile to brittle while localizing below the dark marble level. The Schmidt's lower hemisphere equal-area projections show the concordance of the direction of extension in ductile and brittle structures.

than 10 cm. However, in the most deformed levels, it can reach 10 m. In the hanging wall of the shear zones, small top-to-the-north reverse faults develop when the thickness of the shear zones diminishes (Figures 11c and 12). They are interpreted as accommodation structures of the top-to-the-north displacements when the shear zone is partially locked.

[36] Three large top-to-the-north shear zones (SZ) have been observed within the northern part of the Cycladic Blueschists. They are parallel to the schistosity and located between thick marble layers and thick schists layers (Figure 2a). Two of them have been followed along about 2 km: the Homer's tomb shear zone outcropping in the center of the unit (Figure 12) and the Kambaki shear zone outcropping on the northwestern coast (Figure 13). However, all of them could actually be longer. Since they strike parallel to the schistosity, we could not quantify the amount of displacement along them.

[37] Through the Homer's tomb shear zone, four lithologic zones have been distinguished along strike with different structural characteristics (Figure 12). The zones have been correlated on three cross sections. Zone I is composed of thin

layers of schists and marble exhibiting thin top-to-the-north C' -type cleavage and small-scale shear bands parallel to the schistosity. Zone II is a variably deformed marble level. On cross section 1, the marble level appears as a large sigmoid indicating a top-to-the-north sense of shear. On the other cross sections, the deformation in zone II is accommodated by cataclastic flow (cross section 2) and breccia formation (cross section 3). The difference between the three modes of deformation might correspond to variable amounts of strain accommodated by the marble level. Zone III consists in blueschist facies metabasites partially retrogressed in the greenschist facies. Top-to-the-north shearing deformation is accommodated by C' -type cleavage and cataclastic north dipping faults (Figure 12). Zone IV is composed by slightly deformed thick bedded marbles. The evolution of deformation from zone IV to zone I exhibits a gradient of shear accompanied by a gradient of greenschist retrogression. A few normal faults affect zones I, II and III on cross section 2. One brittle slickenside has also been measured on cross section 1. These brittle structures are consistent with a NW–SE direction of extension. We do not explain the

deviation between the ductile and the brittle direction of extension.

[38] The Kambaki shear zone has been divided into four parts (Figure 13). From bottom to top we distinguished chlorite schists, greenschists, orange cataclasites, and dark thick bedded marble.

[39] The chlorite schists average dip is 40° to the north. They are ductilely deformed by a C' -type cleavage. The shear planes are very steep; they dip 80° to the north. They are associated to pull-apart like veins (Figure 11b). In this zone, top-to-the-north deformation is associated to dilatancy. The chlorite schists are highly deformed by folds with axes parallel to the lineation and axial planes parallel to the schistosity (Figure 13). The average dip of the greenschists is 30° to the north. The intense ductile deformation led to grain size reduction and mylonitization. Brittle conjugated normal faults affect the greenschists, with dominant north dipping faults. The faults are associated to joints. The maximal principal stress deduced from these brittle structures is not vertical but roughly perpendicular to the schistosity. This pattern implies temporal or special rotation of the stress ellipsoid. The protolith of the orange cataclasite appears in areas where deformation is less intense. It is the same fine-grained greenschist as the one outcropping below. The average dip is 20° to the north. A few shear criteria indicate a top-to-the-north sense of shear. Joints crosscut the cataclastic schistosity perpendicularly. The dark thick bedded marbles are very lightly deformed. Metabauxite pods are preserved in it.

[40] Below the upper marble level, the distribution of deformation pattern highlights a deformation gradient in the ductile field (from shear bands to mylonites) and in the brittle field (from conjugated normal faults to cataclasites). The deformation gradients are accompanied by a decrease of the schistosity dip (Figure 12).

[41] Compared to the Homer's tomb and the Kambaki shear zones, the third top-to-the-north SZ is poorly developed. Along it, we also observed intense top-to-the-north deformation associated to cataclasites and heterogeneous deformation depending on the lithology (Figures 10c and 10d).

[42] The three top-to-the-north SZ share major structural characteristics. They are the result of localization of the top-to-the-north deformation through 20 to 40 m thick intensely sheared corridors. They also concentrate clearly brittle structures and structures that exhibit both ductile and brittle characteristics. All the structures have roughly the same direction and asymmetry. Moreover, both brittle and ductile structures that form the SZ are apparently extensional. As a result, the shear zones have then accommodated top-to-the-north extension continuously from the ductile field up to the brittle field. The brittle increments of deformation are, nevertheless, poorly developed. It must be noted that the top-to-the-north shear zones develop only in the northern part of the Cycladic Blueschists where the schistosity dips to the north and that they use lithologic heterogeneities to localize the deformation. In the southern part of the Cycladic Blueschists, no such shear zone has been observed and the top-to-the-north criteria are sparse. Furthermore, a few points must be emphasized. The top-to-the-north deformation inten-

sifies in the vicinity of the shear zones. It is also particularly developed between the Homer's tomb SZ and the Kambaki SZ. Below the Homer's tomb SZ, top-to-the-north criteria are scattered. Last, in cross section the schistosity delineates kilometric top-to-the-north sigmoids between the shear zones.

7.2. Evidence and Distribution of Top-to-the-North Deformation in the Cycladic Basement

[43] In the Cycladic Basement garnet-micaschists, the top-to-the-north criteria are the same as those in the Cycladic Blueschists. However, we did not observe shear zones as large and localized as those in the Cycladic Blueschists.

[44] Two kinds of top-to-the-north structures have been recognized. They can clearly be distinguished by their degree of penetrativity. In the levels where deformation intensity associated to top-to-the-south deformation corresponds to the B and C strain facies, the augengneiss sometimes exhibit a pervasive constrictional fabric. This fabric is defined by a poorly developed schistosity and strongly stretched K-feldspar rods. In these augengneiss, constriction tends to produce symmetrical rods. However, asymmetric fabrics have also been observed; they indicate top-to-the-north sense of shear.

[45] Localized structures are also associated to top-to-the-north deformation. The northern part of the orthogneiss is affected by a few north dipping shear zones (Figure 10a). Their dip is between 45° and 70°, and their thickness is between 1 and 20 m. They are formed by close shear planes that define a pervasive fabric. However, the pervasive fabric is restricted to the shear zone. The corresponding strain facies is C; locally, mylonitic fabrics can be found. In these zones, the K-feldspar often deforms brittlely (Figure 10d). The southern part of the orthogneiss is lightly affected by very localized N shear bands. Their dip is very shallow (10–15° to the north) and their thickness is less than 1 cm.

7.3. Metamorphic Conditions of the Top-to-the-North Event

[46] The metamorphic conditions associated to the top-to-the-north deformation have been examined according to the method explained in section 6.3.

[47] In the Cycladic Blueschists, the metabasites that are deformed by top-to-the-north deformation exhibit greenschist facies or strongly retrogressed blueschist facies (Figures 9d and 9e), with only one exception. Moreover, structurally above the Homer's tomb shear zone, the domination of top-to-the-N shear criteria coincides with a strong retrogression in the greenschist facies (Figure 12). At microstructural scale, top-to-the-north structures are associated to low-grade minerals (Figures 6c–6f). The dominant paragenesis in the top-to-the-north shear bands is chlorite-phengite-albite ± biotite. In thin section, albite porphyroblasts are synkinematic (Figure 6f). They are surrounded by quartz-phyllsilicate strain shadows, and they sometimes bear sigmoidal phyllosilicates inclusions. When the HP-LT garnets are preserved from full retrogression, they are destabilized into a chlorite rim that can be asymmetric. On most outcrops, these microstructural criteria indicate a top-to-the-north sense of shear. The evolution from ductile to brittle in

the two units is also a good indicator for the metamorphic conditions of the top-to-the-north deformation. This evolution shows that both units crossed the brittle-ductile transition (BDT), i.e., reached the upper part of the crust, in a top-to-the-north context.

8. Relative Chronology Between Top-to-the-South and Top-to-the-North Events

[48] On the basis of the structural and the metamorphic observations described above, two successive deformation events can be distinguished on Ios island: a top-to-the-south episode and a top-to-the-north episode. In this section, we detail the chronologic evidence that allows a relative timing in the history of the southern Cyclades.

[49] On most outcrop, when the two senses of shear are present, it is almost impossible to define a clear chronology. In these cases, we indicated a double-headed arrow on the lineation map (Figure 3). However, a few continuous and long outcrops exhibit clear crosscutting criteria. Top-to-the-south shear criteria can be preserved within the top-to-the-north extensional shear zones (Figure 8). The Homer's tomb shear zone also provides examples of chronology (Figure 12). In the less deformed metabasites of zone III, fine top-to-the-south criteria are preserved in the footwall of the top-to-the-north structures. Finally, in the Cycladic Basement, the top-to-the-north deformation associated to the top-to-the-south anastomosed shear bands can clearly be distinguished from top-to-the-north normal shear zones (Figure 10). Moreover, the top-to-the-north shear zones clearly crosscut the previous structures.

[50] The same chronology can be inferred from the association between the deformation structures and the metamorphic facies. As emphasized above, in the Cycladic Blueschists, the localization of top-to-the-north deformation in shear zones is associated to deformation gradients (Figures 12 and 13). The examples of preserved blueschist facies parageneses are rare. However, in these cases, the deformation induces retrogression in the greenschist facies (Figures 9 and 12). The deformation gradients associated to top-to-the-north deformation are then closely linked to retrogression gradients in the greenschist facies. The association of retrogression in the greenschist facies and top-to-the-north deformation on the one hand, and blueschist facies metamorphism and top-to-the-south deformation on the other hand also shows that top-to-the-north deformation followed top-to-the-south deformation. Moreover, the evolution from brittle to ductile associated to top-to-the-north shear zones indicates that the BDT has been crossed during top-to-the-north shearing. The last deformation episode is then the top-to-the-north one.

[51] The relative distribution of deformation criteria (Figure 3a) and metamorphic assemblages (Figure 4a) shows a strong correlation. The northern limit of HP-LT parageneses preservation corresponds to the northern limit of the top-to-the-south criteria. The HP-LT assemblages and the top-to-the-south criteria are then structurally restricted in a band between the Cycladic Blueschists–Cycladic Basement contact and the Homer's tomb shear zone. This pattern could be

interpreted as a gradient of top-to-the-south deformation associated to the Cycladic Blueschists–Cycladic Basement contact. However, we interpret it as a gradient of top-to-the-north deformation at the island scale preserving a zone of pristine top-to-the-south shearing. Indeed, above the Homer's tomb shear zone, the top-to-the-north deformation is systematic, whereas below this structure, it coexists with top to the south criteria. Then, top-to-the-north deformation intensifies toward the upper part of the Cycladic Blueschists unit in the northern part of Ios and tends to erase previous structures. Moreover, blueschist facies rocks and the top-to-the-south deformation criteria are present in structures preserved from top-to-the-north deformation (HP-LT metabasites boudins, for example) or where the top-to-the-north deformation is poorly expressed. Thus, the gradient of top-to-the-north deformation and greenschist facies retrogression is linked to a decrease of preservation of top-to-the-south structures and HP-LT parageneses from south to north.

9. Discussion

[52] Our new field data allow us to reconsider the tectonic model for Ios and the Cyclades.

9.1. Significance of the Structures and the Deformation Events

9.1.1. Origin of Top-to-the-South Cycladic Blueschists–Cycladic Basement Contact

[53] The contact between the upper Cycladic Blueschists unit and the lower Cycladic Continental Basement unit is associated with top-to-the-south movements. The related deformations have been recorded in both units. Our observations thus confirm the general kinematics proposed by previous authors [Lister *et al.*, 1984; Vandenberg and Lister, 1996; Forster and Lister, 1999a]. However, the significance of this top-to-the-south kinematics is to be discussed. In the Cycladic Blueschists unit, the top-to-the-south deformation was active in blueschist and in subsequent greenschist facies conditions (Figure 6e). It then initiated in blueschist facies conditions. This statement has already been suggested but no evidence has been provided [Forster and Lister, 1999a]. It has also been shown that blueschist facies conditions are retrograde and postdate the eclogitic peak of pressure [Forster and Lister, 1999b]. Synkinematic retrogression of eclogites in blueschist facies conditions has already been described in the Cyclades on Syros and Sifnos islands [Trotet *et al.*, 2001a, 2001b]. It is classically interpreted as the evidence of exhumation in the subduction zone, coeval with convergent boundary conditions. The top-to-the-south deformation was thus active within the subduction zone, in synorogenic conditions.

[54] Available geochronological studies provide ages between 40 and 50 Ma for the HP-LT conditions [van der Maar and Jansen, 1983; Baldwin, 1996]. The top-to-the-south episode then began at least before 40 Ma. Metamorphic and chronologic constraints for the end of this episode in greenschist facies conditions are less obvious. In the Cycladic Basement unit, ages between 40 and 50 Ma have also been interpreted as the ages of the peak metamorphism [van der

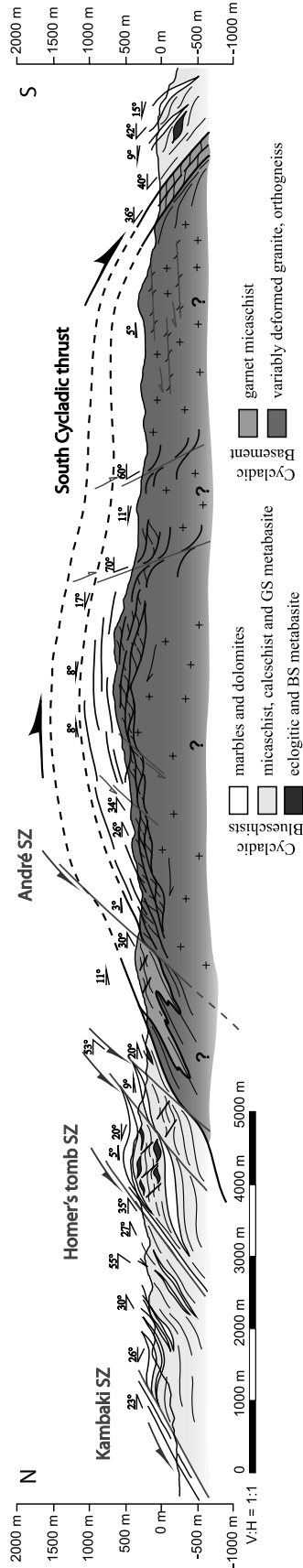


Figure 14. N–S cross section of Ios island. The contact between the Cycladic Blueschists and the Cycladic Basement is a thrust (the south Cycladic thrust) associated to top-to-the-south deformation. In the Cycladic Blueschists, top-to-the-south structures and blueschist facies rocks are preserved in the southern part of the unit and between the extensional shear zones, where the top-to-the-north deformation is less intense. In the Cycladic Basement, the top-to-the-south movements induced a vertical strain gradient. The stretching rises from the core, where the granite is preserved, to the rim, where it is fully mylonitized. In both units, the top-to-the-north extensional deformation is located in large shear zones that deform the previous structures.

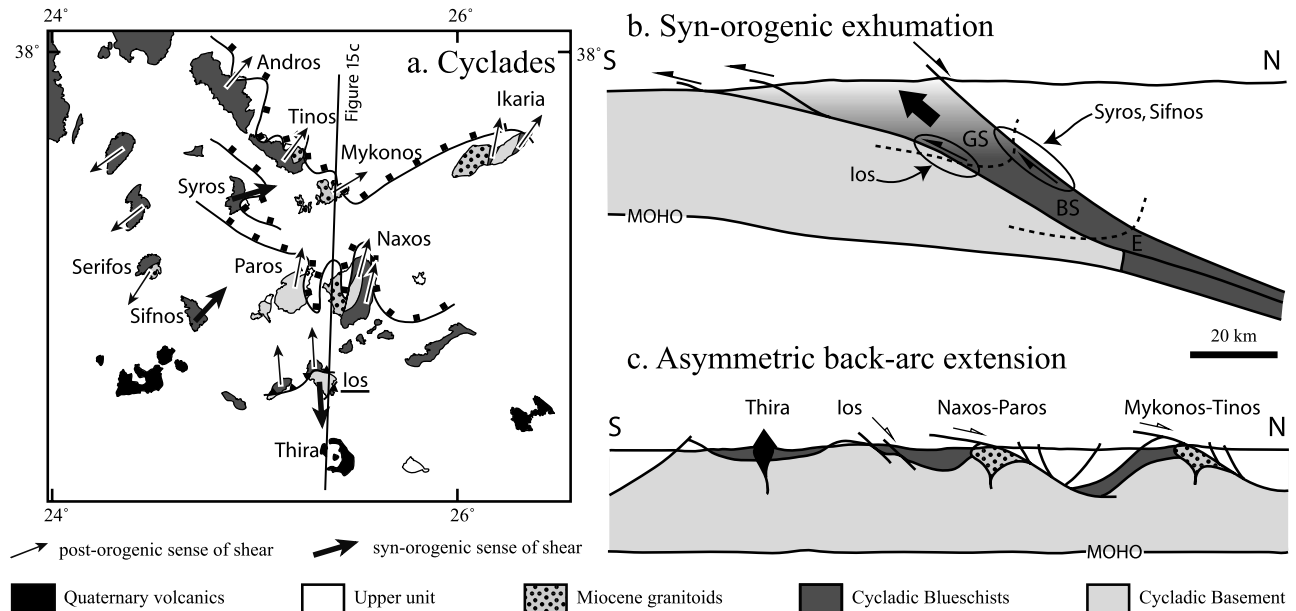


Figure 15. (a) Tectonic map of synorogenic and postorogenic structures in the Cyclades, modified after Jolivet *et al.* [2004b]. The thin arrows indicate the ductile sense of shear associated to the Oligo-Miocene extensional episode [Lister *et al.*, 1984; Faure *et al.*, 1991; Gautier and Brun, 1994b, 1994a; Vandenberg and Lister, 1996; Forster and Lister, 1999a; Jolivet and Patriat, 1999; Mehl *et al.*, 2005, 2007; M. Müller *et al.*, presented paper, 2006; C. Rambousek *et al.*, presented paper, 2006; K. Voit *et al.*, presented paper, 2006]. On Ios island, the postorogenic sense of shear is top-to-the-north. The thick arrows indicate the sense of shear associated to synorogenic exhumation. On Syros and Sifnos islands, the synorogenic sense of shear is top-to-the-east-NE; it is associated to the synorogenic detachment of Syros [Trotet *et al.*, 2001a, 2001b]. On Ios island, synorogenic exhumation is associated to a top-to-the-south thrust. On these three islands, synorogenic deformation evolves from blueschist to greenschist facies conditions. (b) Proposed model for synorogenic exhumation of the Cycladic Blueschists. Its upper limit is a top-to-the-north synorogenic detachment and its lower one is a top-to-the-south thrust. The Cycladic Blueschists unit is exhumed as a whole between the two structures. The metamorphic facies are indicated as GS (greenschist), BS (blueschist), and E (eclogite). (c) Proposed model for back-arc extension in the Cyclades. Extension is asymmetric. It is dominated by top-to-the-north structures that allow the exhumation of the middle and lower crust.

Maar and Jansen, 1983; Andriessen *et al.*, 1987; Baldwin, 1996; Baldwin and Lister, 1998]. The Cycladic Blueschists–Cycladic Basement contact is associated to deformations that began in blueschist facies conditions and ended in greenschist facies conditions. This contact did not show any evolution toward brittle deformation associated to top-to-the-south kinematics. Moreover, the contact allows the juxtaposition of a unit metamorphosed in eclogitic conditions above a unit metamorphosed in lower pressure conditions. We then propose that the Cycladic Blueschists–Cycladic Basement contact is a thrust active in the subduction zone in HP-LT conditions: the south Cycladic thrust (Figures 14, 15a, and 15b). The final juxtaposition of the two units is posterior to the peak of pressure in the Cycladic Blueschists unit. This could explain why pervasive HP-LT parageneses are not clearly recorded in the Cycladic Basement. This proposition contrasts with the interpretation of the contact as a major detachment [Lister *et al.*, 1984; Vandenberg and Lister, 1996; Forster and Lister, 1999a].

[55] The interpretation of the basal contact of the Cycladic Blueschists unit as a thrust with a top-to-the-south/top-to-the-southwest kinematics has also been proposed in the Olympos-Ossa-Pelion region [Godfriaux and Ricou, 1991; Schermer, 1993; Lacassin *et al.*, 2007], on Evia [Ring *et al.*, 2007a], and on Samos [Ring *et al.*, 2007b]. Moreover, the proposition that the Cycladic Blueschists–Cycladic Basement contact is a synorogenic thrust is consistent with paleogeographic data. Indeed, the Cycladic Blueschists is a unit of oceanic affinity that is supposed to belong to the Pindos basin [Bonneau, 1982] and the Cycladic Basement is a unit of continental affinity that is supposed to have been part of the southern margin of the Pindos basin [Jolivet *et al.*, 2004b]. The southward thrust of the basin on its southern margin is consistent with a north dipping subduction.

9.1.2. Effects of the Top-to-the-North Shear Zones

[56] The top-to-the-north deformation exhibits a strain gradient toward the north. This gradient is coeval with a

retrogression gradient in greenschist facies conditions. A similar gradient of noncoaxial strain and retrogression has been observed on Tinos Island below the top-to-the-north detachment [Parra *et al.*, 2002]. It is interpreted as the expression of progressive localization that ends with the formation of the brittle detachment allowing the final exhumation during the postorogenic episode.

[57] On Ios, the ductile top-to-the-north deformation localizes in extensional shear zones in the northern flank of the dome (Figure 14). Five of them have been recognized among which the three largest ones have precisely been documented: from north to south, the Kambaki shear zone (Figure 13), the Homer's tomb (Figure 12) and the Andre shear zones (Figure 3a). Their dips increase from north ($\sim 25^\circ$) to south ($\sim 50^\circ$). In the Cycladic Blueschists unit, they reactivate lithologic heterogeneities but the Cycladic Blueschists–Cycladic Basement contact is crosscut by the southernmost one. In the southern part of the Cycladic Basement, two steeply dipping top-to-the-south normal shear zones have been recognized (Figure 14). We propose that they are associated to the same extensional episode. They could be minor antithetic structures associated to the dominant top-to-the-north asymmetric extension. The brittle direction and asymmetry of extension are roughly the same as the ductile deformation in the top-to-the-north shear zones. This evolution, also recognized on Andros [Mehl *et al.*, 2007] and Tinos [Mehl *et al.*, 2005], has been interpreted as an evidence of continuous extension in the middle and the upper crust. The final exhumation across the brittle-ductile transition is then associated to asymmetric extension dominated by top-to-the-north deformation. Since the top-to-the-north shear zones crosscut the Cycladic Blueschists–Cycladic Basement contact, they necessarily postdate it. This observation is not compatible with the suggestion that they could be antithetic structures of the southward contact between the Cycladic Blueschists and the Cycladic Basement [Forster and Lister, 1999a]. The final part of exhumation is then associated to top-to-the-north deformation.

[58] Yet, our observations show that the top-to-the-north shear zones are not directly responsible for a large exhumation. First, they affect the entire stack and do not separate these units from a nonmetamorphic upper plate that could be of Pelagonian affinity. Second, the amount of exhumation associated to the five top-to-the-north and two top-to-the-south shear zones can be estimated. According to the apparent offset on the map, the vertical offset of the Andre shear zone is approximated at about 400 m (Figures 3a and 3b). It is the only shear zone for which we can directly measure an offset. If we assume that all the shear zones have offsets of similar magnitude, a maximum total vertical exhumation lower than 3500 m can be estimated for the deepest part of the Cycladic Basement. This value is low compared to the minimal depth of the brittle-ductile transition at which the shear zones were active. Even if the final part of the exhumation is associated to the activation of the extensional shear zones, they cannot be responsible for a large part of the exhumation of the metamorphic units. These top-to-the-north structures cannot be described as a detachment in the strict sense. Indeed, we did not observe any major extensional

shear zone similar to those described on Andros [Mehl *et al.*, 2007], Tinos [Patriat and Jolivet, 1998; Mehl *et al.*, 2005], Mykonos [Faure *et al.*, 1991], Naxos [Buick, 1991; Gautier *et al.*, 1993], or Paros [Gautier *et al.*, 1993]. If such a structure exists, it has to be present offshore north of Ios island.

[59] The clear relative timing between the top-to-the-south and top-to-the-north episodes is yet to be confirmed by geochronological work. Nevertheless, Oligo-Miocene ages associated to the LP-HT episode have been obtained [Henjes-Kunst and Kreuzer, 1982; van der Maar and Jansen, 1983; Baldwin, 1996; Baldwin and Lister, 1998]. The top-to-the-north asymmetric extension observed on Ios island is characterized by greenschist facies and brittle conditions. We then suggest that these structures are related to the Oligo-Miocene extensional episode. Low-temperature geochronological data provide constraints for the end of the exhumation on Ios island [Brichau, 2004]. This study points out an apparent younging of zircon FT ages (14.5 ± 1.6 to 13.5 ± 1.4 Ma), apatite FT ages (12.2 ± 1.4 to 11.0 ± 1.4 Ma) and apatite U-Th-He (10.8 ± 1.0 to 9.5 ± 0.8 Ma) ages northward in the Cycladic Basement. These values indicate a final exhumation in the lower Miocene. Moreover, the apparent northward younging is consistent with the exhumation below top-to-the-north structures.

9.2. Implications for the Dynamic of the Aegean Subduction Zone

[60] On most Cycladic islands (Figure 15a), the Oligo-Miocene extensional reworking of the nappe stack erased most of the Eocene kinematic indicators [Jolivet *et al.*, 2004b]. However, on Syros and Sifnos islands the synorogenic kinematics is preserved. On both islands, the deformation is characterized by top-to-the-east-northeast deformation (Figure 15a) active in blueschist facies and greenschist facies conditions [Trotet *et al.*, 2001a, 2001b]. The deformation is localized on the synorogenic detachment exposed on Syros. This structure associated to extensional deformation separates the Cycladic Blueschists unit and the upper non-HP Pelagonian unit. During the early exhumation in blueschist and greenschist facies conditions, the upper contact of the Cycladic Blueschists unit was an extensional structure associated to top-to-the-east-northeast movements in the present-day configuration. The western Cycladic islands (comprising Syros and Sifnos) experienced a clockwise rotation after the Middle Miocene, the magnitude of which cannot be determined, whereas the eastern Cycladic islands (comprising Ios) are supposed to have experienced limited rotation [Morris and Anderson, 1996; van Hinsbergen *et al.*, 2005]. The Eocene sense of shear during the synorogenic period is reconstructed by canceling the post-Eocene rotation: it corresponds to top-to-the-north-NE movements. On Ios island, we have shown that the basal contact of the Cycladic Blueschists unit is an Eocene thrust active in blueschist and then greenschist facies conditions. Thus, in Eocene synorogenic times the Cycladic Blueschists unit was limited by a top-to-the-north-NE detachment at its top and by a top-to-the-south thrust at its bottom. This pattern defines an extrusion structure that operates in the subduction zone during the early

exhumation in blueschist and greenschist facies conditions (Figure 15b). Such extrusion structures with similar kinematics have been described for the Cycladic Blueschists unit in the Olympos-Ossa-Pelion region [Lacassin *et al.*, 2007], on Evia island [Ring *et al.*, 2007a] and on Samos island [Ring *et al.*, 2007b]. However, the basal unit below the Cycladic Blueschists is not the Cycladic Basement for those three regions. It has been suggested that the early exhumation of the Cycladic Blueschists unit in blueschist and greenschist facies conditions is due to an extrusion wedge on Evia and Samos islands [Ring *et al.*, 2007a, 2007b]. We propose that a continuous extrusion structure existed during the Eocene from the Olympos region in the west to Samos island in the east. This structure would have accomplished the exhumation of the Cycladic Blueschists unit along the whole subduction zone.

[61] The description of asymmetric postorogenic extension on Ios, largely dominated by top-to-the-north movements, allows a reappraisal of the regional kinematics during the Oligo-Miocene collapse episode. The MCCs of the northern and the central Cyclades exhibit top-to-the-north movements in the lower plate (Figure 15a). The top-to-the-south deformation described in the western Cyclades (Figure 15a) [Grasemann and Petrakakis, 2007] is partly posterior to the Serifos intrusive that yielded ages between 8 and 9 Ma [Iglseider *et al.*, 2009]. LT chronology indicates that at this time the northern, the central and the southern Cyclades were almost totally exhumed [Brichau, 2004; Brichau *et al.*, 2008]. The top-to-the-south extensional deformation observed in the western Cyclades partly post-dates the top-to-the-north deformation observed elsewhere in the Archipelago. One additional point must be considered: the top-to-the-south kinematic indicators observed in Kea, Kithnos and Serifos are not associated with the presence of a detachment. No outcrop of the upper Cycladic unit is preserved on these islands and thus the top-to-the-south kinematics cannot be unambiguously associated with a major extensional structure. Whether they are associated in time, at least partly, to the top-to-the-north shear sense seen in the northern Cyclades is a point that remains to be specified. If they are partly contemporaneous they could be conjugate structures to the major detachments seen further north accommodating internal deformation within the lower and middle crust. The ascertained major extensional structures are thus top-to-the-north detachments. Even if the stretching pattern is disturbed by rotations in the upper crust in the Cyclades [van Hinsbergen *et al.*, 2005], the general shear sense is top-to-the-north in most of the northern and central Cyclades. This pattern indicates that the back-arc north-south extension was asymmetric (Figure 15c). In the northern and the central Cyclades it was accommodated by two crustal-scale top-to-the-north shear zones. On Ios, even if no detachment is exposed, the extensional shear zones indicate the same asymmetry. At regional scale, extensional collapse was then controlled by a significant component of simple shear, with no major antithetic structures accommodating rotation between the shear zones.

[62] Regional asymmetry displayed by the sense of ductile shear is a major characteristic shared by the three back-arc

domains of the Mediterranean: the Alboran, the Tyrrhenian and the Aegean regions (Figure 1a). Two types of driving forces have been proposed to induce the thinning of a thickened lithosphere: gravity forces and tensional forces [Rey *et al.*, 2001]. We suggest that gravitational spreading of the thickened continental lithosphere under its own weight alone would have led to a more symmetrical structure. Furthermore gravitational spreading is permitted by an active component of slab retreat [Jolivet and Patriat, 1999; Jolivet and Faccenna, 2000].

[63] Moreover, asymmetry is directed toward the trench in the Tyrrhenian and the Alboran regions, whereas it is directed away from the trench in the Aegean domain [Jolivet *et al.*, 2008]. At least two different processes must exist and combine their actions with gravity in order to induce asymmetric extension at regional scale toward and away from the trench. Several models have been proposed in order to explain these observations in the case of the Aegean back-arc region: (1) the crust is rheologically anisotropic: detachments reactivate oblique structures such as thrusts inherited from the compressional episodes [Le Pourhiet *et al.*, 2004]; (2) a vertical coupling in the back-arc lithosphere exists between the crust and the mantle: simple shear at the crustal scale would be bottom-driven by a basal drag in the mantle [Jolivet *et al.*, 2008; Tikoff *et al.*, 2004]; (3) the lateral variation of basal heat flux in the lithosphere induces rheological weaknesses in which the detachments root [Le Pourhiet *et al.*, 2003].

[64] In the case of the Aegean asymmetric extension, these different models have to be tested by numerical experiments constrained by accurate P-T-t deformation data.

10. Conclusion

[65] Ios island is a key locality to determine the extensional pattern of back-arc extension in the Cyclades. There, two successive deformation episodes with distinct characteristics can be distinguished.

[66] The top-to-the-south episode is associated to the contact between the Cycladic Blueschists unit and the Cycladic Continental Basement. In the Cycladic Blueschists, it is associated to pervasive and homogeneous deformations in blueschist to greenschist facies conditions. In the Cycladic Basement, it led to the formation of a vertical strain gradient in greenschist facies conditions. The contact between the two units is not an extensional structure [Lister *et al.*, 1984; Vandenberg and Lister, 1996; Forster and Lister, 1999a] but a south directed thrust. It separates a unit of oceanic affinity metamorphosed with eclogite facies relicts in the hanging wall from a unit of continental affinity metamorphosed in lower grade conditions in the footwall. The top-to-the-north episode is characterized by large extensional shear zones acting during exhumation across the brittle-ductile transition. Extensional deformation is controlled by top-to-the-north shear zones that crosscut the whole metamorphic stack. No detachment with a nonmetamorphic unit at its hanging wall can be inferred on Ios.

[67] These local conclusions have major implications concerning the dynamic of the Aegean domain. We thus

propose the following statements. The base of the Cycladic Blueschists unit is a top-to-the-south thrust that was active within the subduction zone in HP-LT conditions. Combined with the top-to-the-north synorogenic detachment of Syros, this south Cycladic Thrust defines an extrusion structure that allowed the exhumation of the Cycladic Blueschists unit in the Eocene from blueschist or eclogite facies conditions until greenschist facies conditions. Oligo-Miocene back-arc extension in the Cyclades was controlled by simple shear in

the middle and lower crust. All the major ductile extensional structures along a N–S transect where brittle detachments are present are asymmetric and dip to the north. The tectonic significance of such an asymmetry remains to be explained.

[68] **Acknowledgments.** This research is a contribution to the ANR-EGEO project. The GMT software package [Wessel and Smith, 1995] was used in the preparation of this paper. Reviews by B. Grasemann and O. Vanderhaeghe helped improving the manuscript.

References

- Andriessen, P. A. M. (1991), K-Ar and Rb-Sr age determinations on micas of impure marbles of Naxos, Greece: The influence of metamorphic fluids and lithology on the blocking temperature, *Schweiz. Mineral. Petrogr. Mitt.*, **71**, 89–99.
- Andriessen, P. A. M., G. Banga, and E. H. Hebeda (1987), Isotopic age study of pre-Alpine rocks in the basal units on Naxos, Sikinos and Ios, Greek Cyclades, *Geol. Mijnbouw*, **66**, 3–14.
- Aubouin, J., and J. Dercourt (1965), Sur la géologie de l'Egée: Regard sur la Crète (Grèce), *Bull. Geol. Soc. Fr.*, **7**, 787–821.
- Augier, R., L. Jolivet, and C. Robin (2005), Late orogenic doming in the eastern Betic Cordilleras: Final exhumation of the Nevado-Filabride complex and its relation to basin genesis, *Tectonics*, **24**, TC4003, doi:10.1029/2004TC001687.
- Avigad, D., and Z. Garfunkel (1989), Low-angle faults above and below a blueschist belt: Tinos Island, Cyclades, Greece, *Terra Nova*, **1**, 182–187, doi:10.1111/j.1365-3121.1989.tb00350.x.
- Avigad, D., and Z. Garfunkel (1991), Uplift and exhumation of high-pressure metamorphic terranes: The example of the Cycladic blueschists belt (Aegean Sea), *Tectonophysics*, **188**, 357–372, doi:10.1016/0040-1951(91)90464-4.
- Avigad, A., Z. Garfunkel, L. Jolivet, and J. M. Azañón (1997), Back-arc extension and denudation of Mediterranean eclogites, *Tectonics*, **16**, 924–941, doi:10.1029/97TC02003.
- Baldwin, S. L. (1996), Contrasting P-T-t histories for blueschists from the western Baja Terrane and the Aegean; effects of synsubduction exhumation and backarc extension, in *Subduction: Top to bottom*, *Geophys. Monogr.*, vol. 96, edited by G. E. Bebout et al., pp. 135–141, AGU, Washington, D. C.
- Baldwin, S. L., and G. S. Lister (1998), Thermochronology of the South Cyclades Shear Zone, Ios, Greece; effects of ductile shear in the argon partial retention zone, *J. Geophys. Res.*, **103**, 7315–7336, doi:10.1029/97JB03106.
- Bonneau, M. (1982), Evolution géodynamique de l'arc égéen depuis le Jurassique Supérieur jusqu'au Miocène, *Bull. Soc. Geol. Fr.*, **7**, 229–242.
- Bonneau, M. (1984), Correlation of the Hellenic nappes in the south-east Aegean and their tectonic reconstruction, in *The Geological Evolution of the Eastern Mediterranean*, edited by J. E. Dixon and A. H. F. Robertson, pp. 517–527, Blackwell Sci., Oxford, U. K.
- Bonneau, M., and J. R. Kienast (1982), Subduction, collision et schistes bleus: L'exemple de l'Egée (Grèce), *Bull. Soc. Geol. Fr.*, **24**, 785–791.
- Bonneau, M., J. Kienast, C. Lepvrier, and H. Maluski (1980), Tectonique et métamorphisme haute pression d'âge Eocène dans les Hellénides: Exemple de l'île de Syros (Cyclades, Grèce), *C. R. Acad. Sci., Ser. D*, **291**, 171–174.
- Brichau, S. (2004), Constraining the tectonic evolution of extensional fault systems in the Cyclades (Greece) using low-temperature thermochronology, *Ph.D. thesis*, 181 pp., Univ. of Mainz, Mainz, Germany.
- Brichau, S., U. Ring, A. Carter, R. Bolhar, P. Monie, D. Stockli, and M. Brunel (2008), Timing, slip rate, displacement and cooling history of the Mykonos detachment footwall, Cyclades, Greece, and implications for the opening of the Aegean Sea basin, *J. Geol. Soc.*, **165**, 263–277, doi:10.1144/0016-76492006-145.
- Bröcker, M. (1990), Blueschist-to-greenschist transition in metabasites from Tinos island, Cyclade, Greece: Compositional control or fluid infiltration, *Lithos*, **25**, 25–39, doi:10.1016/0024-4937(90)90004-K.
- Bröcker, M., and L. Franz (1998), Rb-Sr isotope studies on Tinos Island (Cyclades, Greece): Additional time constraints for metamorphism, extent of infiltration-controlled overprinting and deformational activity, *Geol. Mag.*, **135**, 369–382, doi:10.1017/S0016756898008681.
- Bröcker, M., D. Bieling, B. Hacker, and P. Gans (2004), High-Si phengite records the time of greenschist facies overprinting: Implications for models suggesting mega-detachments in the Aegean Sea, *J. Metamorph. Geol.*, **22**, 427–442, doi:10.1111/j.1525-1314.2004.00524.x.
- Brunn, J. H., I. Argyriadis, L. E. Ricou, A. Poisson, J. Marcoux, and P. C. de Graciansky (1976), Éléments majeurs de liaison entre Taurides et Hellénides, *Bull. Geol. Soc. Fr.*, **18**, 481–497.
- Buick, I. S. (1991), The late alpine evolution of an extensional shear zone, Naxos, Greece, *J. Geol. Soc.*, **148**, 93–103, doi:10.1144/gsjgs.148.1.0093.
- Crittenden, M. D., P. J. Coney, and G. H. Davis (Eds.) (1980), *Cordilleran Metamorphic Core Complexes*, *Spec. Pap. Geol. Soc. Am.*, vol. 153, 490 pp.
- Davis, G. H., and P. J. Coney (1979), Geological development of metamorphic core complexes, *Geology*, **7**, 120–124, doi:10.1130/0091-7613(1979)7<120:GDOTCM>2.0.CO;2.
- Duchêne, S., R. Aïssa, and O. Vanderhaeghe (2006), Pressure-temperature-time evolution of metamorphic rocks from Naxos (Cyclades, Greece): Constraints from thermobarometry and Rb/Sr dating, *Geodin. Acta*, **19**, 301–321, doi:10.3166/ga.19.301-321.
- Dürr, S., E. Seidel, H. Kreuzer, and W. Harre (1978), Témoins d'un métamorphisme d'âge crétacé supérieur dans l'Egée: Datations radiométriques de minéraux provenant de l'île de Nikouria (Cyclades, Grèce), *Bull. Geol. Soc. Fr.*, **20**, 209–213.
- Faure, M., M. Bonneau, and J. Pons (1991), Ductile deformation and syntectonic granite emplacement during the late Miocene extension of the Aegean (Greece), *Bull. Soc. Geol. Fr.*, **162**, 3–11.
- Forster, M. A., and G. S. Lister (1999a), Detachment faults in the Aegean core complex of Ios, Cyclades, Greece, in *Exhumation Processes: Normal faulting, Ductile Flow and Erosion*, edited by U. Ring et al., *Geol. Soc. Spec. Publ.*, **154**, 305–323.
- Forster, M. A., and G. S. Lister (1999b), Separate episodes of eclogite and blueschist facies metamorphism in the Aegean metamorphic core complex of Ios, Cyclades, Greece, in *Continental Tectonics*, edited by C. Mac Niocall and P. D. Ryan, *Geol. Soc. Spec. Publ.*, **164**, 157–177.
- Gautier, P., and J. P. Brun (1994a), Crustal-scale geometry and kinematics of late-orogenic extension in the central Aegean (Cyclades and Evvia Island), *Tectonophysics*, **238**, 399–424, doi:10.1016/0040-1951(94)90066-3.
- Gautier, P., and J. P. Brun (1994b), Ductile crust exhumation and extensional detachments in the central Aegean (Cyclades and Evvia islands), *Geodin. Acta*, **7**, 57–85.
- Gautier, P., M. Ballèvre, J. P. Brun, and L. Jolivet (1990), Extension ductile et bassins sédimentaires Mio-Pliocène dans les Cyclades (îles de Naxos et de Paros), *C. R. Acad. Sci., Ser.*, **2**, 310, 147–153.
- Gautier, P., J. P. Brun, and L. Jolivet (1993), Structure and kinematics of Upper Cenozoic extensional detachment on Naxos and Paros (Cyclades Islands, Greece), *Tectonics*, **12**, 1180–1194, doi:10.1029/93TC01131.
- Godfriaux, Y., and L. E. Ricou (1991), Direction et sens de transport associés au charriage synmétamorphe sur l'Olympe, *Bull. Geol. Soc. Greece*, **25**, 207–229.
- Grasemann, B., and P. Petrakakis (2007), Evolution of the Serifos Metamorphic Core Complex, *J. Virtual Explor.*, **27**, paper 2, doi:10.3809/jvirtex.2007.00170.
- Grasemann, B., S. Martel, and C. Passchier (2005), Reverse and normal drag along a fault, *J. Struct. Geol.*, **27**, 999–1010, doi:10.1016/j.jsg.2005.04.006.
- Gueydan, F., Y. M. Leroy, L. Jolivet, and P. Agard (2003), Analysis of continental midcrustal strain localization induced by microfracturing and reaction-softening, *J. Geophys. Res.*, **108**(B2), 2064, doi:10.1029/2001JB000611.
- Gupta, S., and M. J. Bickle (2004), Ductile shearing, hydrous fluid channelling and high-pressure metamorphism along the basement-cover contact on Sikinos, Cyclades, Greece, in *Flow Processes in Faults and Shear Zones*, edited by G. I. Alsop et al., *Geol. Soc. Spec. Publ.*, **224**, 161–175, doi:10.1144/GSL.SP.2004.224.01.11.
- Henjes-Kunst, F., and H. Kreuzer (1982), Isotopic dating of pre-alpide rocks from the Island of Ios (Cyclades, Greece), *Contrib. Mineral. Petrol.*, **80**, 245–253, doi:10.1007/BF00371354.
- Iglseder, C., B. Grasemann, D. A. Schneider, K. Petrakakis, C. Miller, U. S. Klötzli, M. Thöni, A. Zámolyi, and C. Rambousek (2009), I and S-type plutonism on Serifos (W-Cyclades, Greece), *Tectonophysics*, doi:10.1016/j.tecto.2008.09.021, in press.
- Jabaloy, A., J. Galindo-Zaldívar, and F. Gonzalez-Lodeiro (1993), The Alpujarride-Nevado-Filabride extensional shear zone, Betic Cordillera, SE Spain, *J. Struct. Geol.*, **15**, 555–569, doi:10.1016/0191-8141(93)90148-4.
- Jacobshagen, V., S. Dürr, F. Kockel, K. O. Kopp, G. Kowalczyk, H. Berckheimer, and D. Büttner (1978), Structure and geodynamic evolution of the Aegean region, in *Alps, Apennines, Hellenides*, edited by H. Cloos et al., pp. 537–564, Int. Union of Geod. and Geophys., Stuttgart, Germany.

- Jansen, J. B. H. (1977), Metamorphism on Naxos, Greece, thesis, Utrecht Univ., Utrecht, Netherlands.
- Jolivet, L., and C. Faccenna (2000), Mediterranean extension and the Africa-Eurasia collision, *Tectonics*, *19*, 1095–1106, doi:10.1029/2000TC900018.
- Jolivet, L., and M. Patriat (1999), Ductile extension and the formation of the Aegean Sea, in *The Mediterranean Basins: Tertiary Extensions Within the Alpine Orogen*, edited by B. Durand et al., *Geol. Soc. Spec. Publ.*, *156*, 427–456.
- Jolivet, L., V. Famin, C. Mehl, T. Parra, D. Avigad, and C. Aubourg (2004a), Progressive strain localisation, crustal-scale boudinage and extensional metamorphic domes in the Aegean Sea, in *Gneiss Domes in Orogens*, edited by D. L. Whitney, C. Teyssier, and C. S. Siddoway, *Spec. Pap. Geol. Soc. Am.*, *380*, 185–210.
- Jolivet, L., G. Rimmelé, R. Oberhänsli, B. Goffé, and O. Candan (2004b), Correlation of syn-orogenic tectonic and metamorphic events in the Cyclades, the Lycian Nappes and the Menderes massif, geodynamic implications, *Bull. Geol. Soc. Fr.*, *175*, 217–238, doi:10.2113/175.3.217.
- Jolivet, L., R. Augier, C. Robin, J.-P. Suc, and J.-M. Rouchy (2006), Lithospheric scale geodynamic context of the Messinian salinity crisis: The Messinian salinity crisis revisited, *Sediment. Geol.*, *188–189*, 9–33, doi:10.1016/j.sedgeo.2006.02.004.
- Jolivet, L., R. Augier, C. Faccenna, F. Negro, G. Rimmelé, P. Agard, C. Robin, F. Rossetti, and A. Crespo-Blanc (2008), Subduction, convergence and the mode of back-arc extension in the Mediterranean region, *Bull. Soc. Geol. Fr.*, *179*, 525–550, doi:10.2113/gssgfbull.179.6.525.
- Katzir, Y., A. Matthews, Z. Garfunkel, M. Schliestedt, and D. Avigad (1996), The tectono-metamorphic evolution of a dismembered ophiolite (Tinos, Cyclades, Greece), *Geol. Mag.*, *133*, 237–254.
- Keay, S., G. Lister, and I. Buick (2001), The timing of partial melting, Barrovian metamorphism and granite intrusion in the Naxos metamorphic core complex, Cyclades, Aegean Sea, Greece, *Tectonophysics*, *342*, 275–312, doi:10.1016/S0040-1951(01)00168-8.
- Lacassin, R., N. Arnaud, P. H. Leloup, R. Armijo, and B. Meyer (2007), Syn- and post-orogenic exhumation of metamorphic rocks in North Aegean, *eEarth*, *2*, 51–63.
- Le Pichon, X., and J. Angelier (1981), The Aegean Sea, *Philos. Trans. R. Soc. London*, *300*, 357–372, doi:10.1098/rsta.1981.0069.
- Le Pourhiet, L., E. Burov, and I. Moretti (2003), Initial crustal thickness geometry controls on the extension in a back arc domain: Case of the Gulf of Corinth, *Tectonics*, *22*(4), 1032, doi:10.1029/2002TC001433.
- Le Pourhiet, L., E. Burov, and I. Moretti (2004), Rifting through a stack of inhomogeneous thrusts (the dipping pie concept), *Tectonics*, *23*, TC4005, doi:10.1029/2003TC001584.
- Lister, G. S., and G. A. Davis (1989), The origin of metamorphic core complexes and detachment faults formed during Tertiary continental extension in the northern Colorado River region, U.S.A., *J. Struct. Geol.*, *11*, 65–94, doi:10.1016/0191-8141(89)90036-9.
- Lister, G. S., G. Banga, and A. Feenstra (1984), Metamorphic core complexes of cordilleran type in the Cyclades, Aegean Sea, Greece, *Geology*, *12*, 221–225, doi:10.1130/0091-7613(1984)12<221:MCCOCT>2.0.CO;2.
- Malavielle, J. (1993), Late orogenic extension in mountain belts: Insights from the Basin and Range and the late Paleozoic Variscan belt, *Tectonics*, *12*, 1115–1130, doi:10.1029/93TC01129.
- Maluski, H., M. Bonneau, and J. R. Kienast (1987), Dating the metamorphic events in the Cycladic area: $^{39}\text{Ar}/^{40}\text{Ar}$ data from metamorphic rocks of the island of Syros (Greece), *Bull. Geol. Soc. Fr.*, *8*, 833–842.
- Martin, L. (2004), Signification des âges U-Pb sur zircon dans l'histoire métamorphique de Naxos et Ikaria (Cyclades, Grèce), thèse de Doctorat, 266 pp., Univ. Henri Poincaré, Nancy, France.
- Martin, L., S. Duchêne, E. Deloule, and O. Vanderhaeghe (2006), The isotopic composition of zircon and garnet: a record of the metamorphic history of Naxos, Greece: Geochronology of orogenic processes, crystal-chemical to continental scale interpretations, *Lithos*, *87*, 174–192, doi:10.1016/j.lithos.2005.06.016.
- Martin, L. A. J., S. Duchêne, E. Deloule, and O. Vanderhaeghe (2008), Mobility of trace elements and oxygen in zircon during metamorphism: Consequences for geochemical tracing, *Earth Planet. Sci. Lett.*, *267*, 161–174, doi:10.1016/j.epsl.2007.11.029.
- Mehl, C., L. Jolivet, and O. Lacombe (2005), From ductile to brittle: Evolution and localization of deformation below a crustal detachment (Tinos, Cyclades, Greece), *Tectonics*, *24*, TC4017, doi:10.1029/2004TC001767.
- Mehl, C., L. Jolivet, O. Lacombe, L. Labrousse, and G. Rimmelé (2007), Structural evolution of Andros (Cyclades, Greece); a key to the behaviour of a (flat) detachment within an extending continental crust, in *The Geodynamics of the Aegean and Anatolia*, edited by T. Taymaz, Y. Yilmaz, and Y. Dilek, *Geol. Soc. Spec. Publ.*, *291*, 41–73.
- Meyre, C., C. D. Capitani, and J. H. Partzsch (1997), A ternary solid solution model for omphacite and its application to geothermobarometry of eclogites from the Middle Adula nappe (central Alps, Switzerland), *J. Metamorph. Geol.*, *15*, 687–700, doi:10.1111/j.1525-1314.1997.00042.x.
- Mitra, G. (1978), Ductile deformation zones and mylonites: The mechanical processes involved in the deformation of crystalline basement rocks, *Am. J. Sci.*, *278*, 1057–1084.
- Morris, A., and A. Anderson (1996), First paleomagnetic results from the Cycladic Massif, Greece, and their implications for Miocene extension directions and tectonic models in the Aegean, *Earth Planet. Sci. Lett.*, *142*, 397–408, doi:10.1016/0012-821X(96)00114-8.
- Parra, T., O. Vidal, and L. Jolivet (2002), Relation between deformation and retrogression in blueschist metapelites of Tinos island (Greece) evidenced by chlorite-mica local equilibria, *Lithos*, *63*, 41–66, doi:10.1016/S0024-4937(02)00115-9.
- Passchier, C. W., and R. A. J. Trouw (2005), *Microtectonics*, 366 pp., Springer, Berlin.
- Patriat, M., and L. Jolivet (1998), Post-orogenic extension and shallow-dipping shear zones, study of a brecciated decollement horizon in Tinos (Cyclades, Greece), *C. R. Acad. Sci., Ser. IIA*, *326*, 355–362.
- Patzak, M., M. Okrusch, and H. Kreuzer (1994), The Akrotiri Unit of the island of Tinos, Cyclades, Greece: Witness to a lost terrane of Late Cretaceous age, *N. Jahrb. Geol. Palaeontol. Abh.*, *194*, 211–252.
- Pe-Piper, G., and D. J. W. Piper (2002), *The Igneous Rocks of Greece*, 573 pp., Borntraeger, Berlin.
- Perraki, M., and E. Mposkos (2001), New constraints for the alpine HP metamorphism of the Ios basement, Cyclades, Greece, *Bull. Geol. Soc. Greece*, *25*, 977–984.
- Platt, J. L., R. Anczkiewicz, J.-I. Soto, S. P. Kelley, and M. Thirlwall (2006), Early Miocene continental subduction and rapid exhumation in the western Mediterranean, *Geology*, *34*, 981–984, doi:10.1130/G22801A.1.
- Rey, P., O. Vanderhaeghe, and C. Teyssier (2001), Gravitational collapse of the continental crust: Definition, regimes and modes, *Tectonophysics*, *342*, 435–449, doi:10.1016/S0040-1951(01)00174-3.
- Ring, U., J. Glodny, T. Will, and S. Thomson (2007a), An Oligocene extrusion wedge of blueschist-facies nappes on Evia, Aegean Sea, Greece: Implications for the early exhumation of high-pressure rocks, *J. Geol. Soc.*, *164*, 637–652, doi:10.1144/0016-76492006-041.
- Ring, U., T. Will, J. Glodny, C. Kumerics, K. Gessner, S. Thomson, T. Güngör, P. Monié, M. Okrusch, and K. Drüppel (2007b), Early exhumation of high-pressure rocks in extrusion wedges: Cycladic blueschist unit in the eastern Aegean, Greece, and Turkey, *Tectonics*, *26*, TC2001, doi:10.1029/2005TC001872.
- Rossetti, F., C. Faccenna, L. Jolivet, F. Tecce, R. Funicello, and C. Brunet (1999), Syn- versus post-orogenic extension in the Tyrrhenian Sea, the case study of Giglio Island (northern Tyrrhenian Sea, Italy), *Tectonophysics*, *304*, 71–93, doi:10.1016/S0040-1951(98)00304-7.
- Schermer, E. R. (1993), Geometry and kinematics of continental basement deformation during the Alpine orogeny, Mt. Olympos region, Greece, *J. Struct. Geol.*, *15*, 571–591, doi:10.1016/0191-8141(93)90149-5.
- Schliestedt, M., R. Altherr, and A. Matthews (1987), Evolution of the Cycladic crystalline complex: Petrology, isotope geochemistry and geochronology, in *Chemical Transport in Metasomatic Processes*, edited by H. C. Helgerson, pp. 389–428, D. Reidel, Dordrecht, Netherlands.
- Schmädicke, E., and T. M. Will (2003), Pressure-temperature evolution of blueschist facies rock from Sifnos, Greece, and implications for the exhumation of high-pressure rocks in the central Aegean, *J. Metamorph. Geol.*, *21*, 799–811, doi:10.1046/j.1525-1314.2003.00482.x.
- Stampfli, M., I. Vavassis, A. De Bono, F. Rossetti, B. Matti, and M. Bellini (2003), Remnants of the Paleotethys oceanic suture-zone in the western Tethyan area: Late Palaeozoic to early Mesozoic events of Mediterranean Europe, and additional regional reports; proceedings, *Boll. Soc. Geol. Ital.*, *2*, 1–23.
- Tikoff, B., R. Russo, C. Teyssier, and A. Tommasi (2004), Mantle-driven deformation of orogenic zones and clutch tectonics, in *Seismic Geomorphology*, edited by R. J. Davies et al., *Geol. Soc. Spec. Publ.*, *227*, 41–64.
- Trotet, F., L. Jolivet, and O. Vidal (2001a), Tectono-metamorphic evolution of Syros and Sifnos islands (Cyclades, Greece), *Tectonophysics*, *338*, 179–206, doi:10.1016/S0040-1951(01)00138-X.
- Trotet, F., O. Vidal, and L. Jolivet (2001b), Exhumation of Syros and Sifnos metamorphic rocks (Cyclades, Greece): New constraints on the P-T paths, *Eur. J. Mineral.*, *13*, 901–920, doi:10.1127/0935-1221/2001/0013/0901.
- Vandenberg, L. C., and G. S. Lister (1996), Structural analysis of basement tectonics from the Aegean metamorphic core complex of Ios, Cyclades, Greece, *J. Struct. Geol.*, *18*, 1437–1454, doi:10.1016/S0191-8141(96)00068-5.
- Vanderhaeghe, O. (2004), Structural record of the Naxos dome formation, in *Gneiss Dome in Orogeny*, edited by D. L. Whitney, C. Teyssier, and C. S. Siddoway, *Spec. Pap. Geol. Soc. Am.*, *380*, 211–227.
- van der Maar, P. (1980), The geology and petrology of Ios, Cyclades, Greece, *Ann. Geol. Pays Helleniques*, *30*, 206–224.
- van der Maar, P., and J. B. H. Jansen (1983), The geology of the polymetamorphic complex of Ios, Cyclades, Greece and its significance for the Cycladic Massif, *Geol. Rundsch.*, *72*, 283–299, doi:10.1007/BF01765910.
- van der Maar, P. A., B. W. Vink, and B. H. Jansen (1981), Ios, geological map, scale 1:50,000, Inst. of Geol. and Miner. Explor., Athens, Greece.
- van Hinsbergen, D. J. J., C. G. Langereis, and J. E. Meulenkamp (2005), Revision of timing, magnitude and distribution of Neogene rotations in the western Aegean region, *Tectonophysics*, *396*, 1–34, doi:10.1016/j.tecto.2004.10.001.
- Wessel, P., and W. H. F. Smith (1995), New version of the Generic Mapping Tools released, *Eos Trans. AGU*, *76*, 329.

Wernicke, B. (1985), Uniform-sense simple shear of the continental lithosphere, *Can. J. Earth Sci.*, *22*, 108–125.

Wijbrans, J. R., and I. McDougall (1986), $^{40}\text{Ar}/^{39}\text{Ar}$ dating of white micas from an alpine high-pressure metamorphic belt on Naxos (Greece): The resetting

of the argon isotopic system, *Contrib. Mineral. Petrol.*, *93*, 187–194, doi:10.1007/BF00371320.

Will, T., M. Okrusch, E. Schmädicke, and G. Chen (1998), Phase relations in the greenschist-blueschist-amphibolite-eclogite facies in the system $\text{Na}_2\text{O}-\text{CaO}-\text{FeO}-\text{MgO}-\text{Al}_2\text{O}_3-\text{SiO}_2-\text{H}_2\text{O}$

(NCFMASH), with application to metamorphic rocks from Samos, Greece, *Contrib. Mineral. Petrol.*, *132*, 85–102, doi:10.1007/s004100050406.

B. Huet, L. Jolivet, and L. Labrousse, iSTEP, UMR 7193, Université Pierre et Marie Curie, CNRS, 4 Place Jussieu, T 46-00 E2, Case 129, F-75252 Paris CEDEX 05, France. (benjamin.huet@upmc.fr)